Spring 2020 – Systems Biology of Reproduction
Discussion Outline – Male Reproductive Tract Development & Function
Michael K. Skinner – Biol 475/575
CUE 418, 10:35-11:50 am, Tuesday & Thursday
February 6, 2020
Week 4

Reproduction Tract Development & Function

Primary Papers:

1. Murashima, et al. (2015) Asian J Andrology 17:749-755
2. Zhao, et al. (2017) Science 357:717-720
3. Liu, et al. (2017) Sexual Development 11:190-202

Discussion

Student 7: Classic Reference #1 above
- What are the developmental steps of the Wolffian/epididymal duct?
- What are the Phenotypes of knockouts that explain the development?
- What technology was used

Student 8: Reference #2 above
- What is the technology used?
- Where is the expression pattern of the COUP-TF11?
- What does the knockout phenotypes show on regional actions of COUP-TF11?

Student 9: Reference #3 above
- What is the technology used?
- What androgen alterations in actin localization were observed?
- What basic information on male reproductive tract development was obtained?

Asian Journal of Andrology (2015) 17, 749–755

www.asiaandro.com; www.ajandrology.com

Open Access

INVITED REVIEW

Sperm Biology

Understanding normal and abnormal development of the Wolffian/epididymal duct by using transgenic mice

Aki Murashima[1], Bingfang Xu[2], Barry T Hinton[2]

The development of the Wolffian/epididymal duct is crucial for proper function and, therefore, male fertility. The development of the epididymis is complex; the initial stages form as a transient embryonic kidney; then the mesonephros is formed, which in turn undergoes extensive morphogenesis under the influence of androgens and growth factors. Thus, understanding of its full development requires a wide and multidisciplinary view. This review focuses on mouse models that display abnormalities of the Wolffian duct and mesonephric development, the importance of these mouse models toward understanding male reproductive tract development, and how these models contribute to our understanding of clinical abnormalities in humans such as congenital anomalies of the kidney and urinary tract (CAKUT).

Asian Journal of Andrology (2015) **17**, 749–755; doi: 10.4103/1008-682X.155540; published online: 26 June 2015

Keywords: epididymis; mesonephros; transgenic mice; Wolffian duct

INTRODUCTION

Understanding the mechanisms that regulate the development of the Wolffian duct (WD) is important because disruption of epididymal function may arise as a consequence of its abnormal development. Very little is known of either the process of WD development or the nature and causes of congenital defects that lead to male infertility. For example, it is clear that an undeveloped initial segment of the epididymis leads to male infertility[1,2] and considering that the human epididymis has an initial segment-like epithelium,[3] it is important to at least understand the development of this region. There are three developmental processes that are considered to be important during the development of the WD: (1) mesonephros formation, (2) stabilization of the ductal system and further growth, (3) postnatal differentiation (**Figure 1**). Each process is dependent upon developmental factors as shown by WD phenotypic mice carrying mutations of each factor.

This review focuses on mouse models that display abnormalities in WD or mesonephric development, the importance of these mouse models toward understanding male reproductive tract development, and how these models contribute to understanding clinical abnormalities in humans. **Table 1** shows mutations of genes in mice that display Wolffian/epididymal duct phenotypes.

DEVELOPMENT OF WOLFFIAN/EPIDIDYMAL DUCT AND MOUSE MODELS

Mesonephros formation

During development, the nephric duct/Wolffian duct (WD) arises from the anterior, intermediate mesoderm, and extends caudally.[4] In the case of mouse, WD formation begins approximately on embryonic day (E) 8.5 and is completed by reaching the cloaca at E9.5[5] (**Figure 1a** and **1b**). As the WD elongates, it induces the formation of nephric tubules through a mesenchymal-epithelial transition process. The tubules form three kidney primordia: pronephros, mesonephros and metanephros[6] (**Figure 1c**). The pronephros and mesonephros are transient kidneys and degenerate soon after their formation. However, in the mesonephros, the WD and cranial mesonephric tubules (MT) are retained and give rise to the male reproductive tract including the epididymis and efferent ducts, respectively.

Because WD formation is crucial for kidney development in mammals, many mouse models that show abnormal WD or mesonephric development also display urogenital abnormalities. The paired domain transcription factors Pax2 and Pax8 are well-known inducers of the initial formation of the WD.[7,8] The LIM-class homeobox gene *Lim1* is required for the extension of the WD.[9,10] Mice carrying a null mutation of *Emx2*, a mouse homologue of the *Drosophila* head gap gene *empty spiracles* (*ems*), display normal WD development until E10.5, but at later time points the duct degenerates, resulting in lack of a kidney and a failure of the reproductive tract to develop.[11] Mice carrying a null mutation of *Gata3*, which is a transcriptional target of Pax2 and Pax8, also show defects in WD initiation.[12]

Growth factors can differentially regulate gene expression especially through epithelial-mesenchymal interactions. Fibroblast growth factor (FGF) signaling is one of the well analyzed growth factor signaling events during mesonephric formation. *Fgf8* encodes an FGF ligand, which is expressed in the intermediate mesoderm, and lack of its expression results in the absence of the cranial mesonephros and MTs.[13]

[1]Department of Developmental Genetics, Institute of Advanced Medicine, Wakayama Medical University, 811-1 Kimiidera, Wakayama 641-8509, Wakayama, Japan; [2]Department of Cell Biology, University of Virginia School of Medicine, Charlottesville, VA 22908, USA.
Correspondence: Prof. Barry T Hinton (bth7c@virginia.edu)
This article was presented at the 6th International Conference on the Epididymis in Shanghai, Oct 31-Nov 3, 2014.

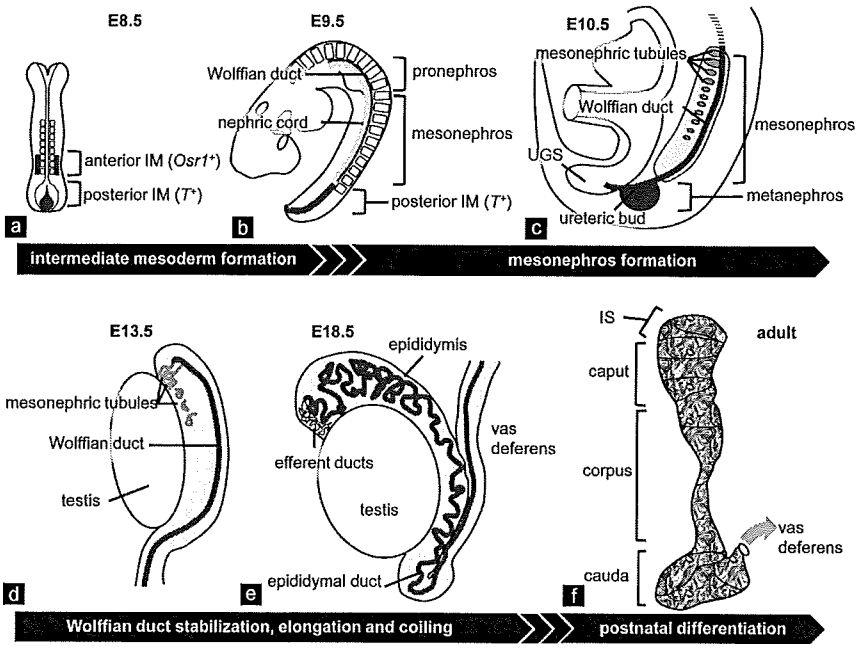

Figure 1: Schematic diagram of mouse Wolffian/epididymal duct development. (**a–c**) The origin of the epididymis is the intermediate mesoderm. Spatiotemporally distinct intermediate mesoderm at E8.5 gives rise to the WD and metanephric mesenchyme.[37] The anterior intermediate mesoderm, which gives rise to the pronephros and the whole WD, is composed of *Osr1*-positive cells at E8.5. The posterior intermediate mesoderm, which gives rise to the metanephric mesenchyme, is positive for *T* at E9.5. The posterior intermediate mesoderm may correspond to axial progenitor cells, which serve as the source of the caudal body trunk.[96,97] The WD begins to form from the anterior intermediate mesoderm at E8.5 and grows posteriorly reaching the urogenital sinus at E9.5.[98] Meanwhile, the pronephros regresses through apoptosis.[99] The WD induces the formation of mesonephric tubules from the mesenchyme (nephric cord) adjacent to the WD in a cranio-caudal manner. At the caudal end of the WD, the metanephros is initiated by ureteric bud formation through the interaction between WD epithelia and the metanephric mesenchyme at E10.5. (**d**) After gonadal sexual differentiation begins, the WD in the female embryo regresses from cranial to caudal while the WD in the male embryo is stabilized. The cranial set of mesonephric tubules connected to the WD is stabilized while the caudal set of mesonephric tubules regresses *via* apoptosis. (**e**) In the male embryo, the stabilized WD begins to coil from the cranial portion at E15.5. The duct continues to elongate and coil throughout development. (**f**) Ductal elongation and coiling continue after birth. The single-layered ductal epithelia undergo differentiation between P15 and P44. At the same time, the regions of the epididymis, initial segment, caput, corpus and cauda, become morphologically distinct. Sperm transport through the duct begins at approximately P35.[59,68] IM: intermediate mesoderm; UGS: urogenital sinus; IS: initial segment.

FGF ligands bind and activate alternatively-spliced forms of four tyrosine kinase FGF receptors (FGFRs 1–4).[14] During mesonephric development, *Fgfr1* is expressed in the mesenchyme while *Fgfr2* is in the epithelium, maintaining the WD and mesonephric mesenchyme.[15] The function of FGFR2 in the WD epithelia is suggested to maintain the caudal part of the WD in the mesonephros by regulating cell proliferation.[16]

Wnt genes encode a family of secreted glycolipoproteins regulating multiple processes during development, including cell proliferation and cell polarity. Among the *Wnt* genes, *Wnt9b* is mainly expressed in the WD epithelium while *Wnt7b* is faintly expressed from E9.5 onward. In animals devoid of *Wnt9b* their MTs are absent, and the epididymis is lacking at birth despite the normal formation of the WD at E10.5.[17] β-catenin-dependent canonical WNT signaling, which mainly regulates cell proliferation and differentiation, is sufficient to rescue MT induction in *Wnt9b* null mice. On the other hand, during metanephric kidney development, attenuation of *Wnt9b* affects the planar cell polarity of the epithelium and lead to tubules with an increased diameter.[18] Further spatiotemporal analyses of epididymal development in this mutant would contribute to our understanding of this molecule in tubulogenesis and its maintenance.

The number of MTs differs between species, and their function as a secretory organ is observed in pigs and humans but not in mice.[19–21] The number of efferent ducts reaching the testis also differs between species.[22,23] It is unclear whether there is a correlation between early MT number and the final number of efferent ducts observed in the adult. MT formation may resemble the formation of the renal nephron; both have the characteristic 'J' or 'S' shape during early development. The nephric tubule is formed through a mesenchymal-to-epithelial transition, and this cellular process is shared between mesonephric and metanephric tubules. *Pax2/8*, *Emx2* and *Lim1* are expressed in the condensed nephric cord and are required for tubulogenesis in addition to WD development.[7–11,24] The Wilms' tumor suppressor gene *Wt-1* and the homeobox gene *Six1* are also expressed in the nephrogenic mesenchymal condensation throughout the nephrogenic cord. Mice lacking *Wt-1* or *Six1* lack caudal MTs while cranial MTs are intact. These observations indicate that the regulation of the cranial and caudal set of MTs is distinct.[25–27] Conversely, lack of the forkhead transcription factors *Foxc1* and *Foxc2*, as well as *Sonic hedgehog* (*Shh*) expressed in the notochord or floor plate, results in supernumerary MT formation, suggesting suppressive effects of these genes on MT formation.[28,29] It is important to uncover how the differential regulation of tubule formation and stabilization along the anterior-posterior axis of the nephrogenic cord is established.

The connection between the rete testis and efferent ducts is observed at E13.5, and testicular fluid transport is detected at the corresponding stage of the rat embryo.[30] The patterning of efferent duct formation is intriguing, but the manner by which they reach the testis is not clear. There are at least two hypotheses on how the efferent ducts could be formed: (1) that a subset of MTs branch and fuse with each other forming the characteristic network of ductules, (2) that branching morphogenesis does not occur and the characteristic

Table 1: Mouse models which show defects in WD/epididymal duct development

Gene	*Type of mutation, Cre driver*	*Phenotype of the mutant*	*References*
Defect in mesonephros formation			
Pax2	KO	Dysgenesis of WD and MD, absence of MT	7
Pax8	KO	Normal	24
Pax2/Pax8	dKO	Dysgenesis of WD and MD, absence of MT	8
Lim1	KO	Dysgenesis of WD	10
	Pax2-Cre	Defect in caudal WD extension	9
Gata3	KO	Dysgenesis of WD and MD, absence of MT	12
Wt-1	KO	Absence of caudal MT	26
Six1	KO	Absence of caudal MT	27
Osr1	KO	Defect in WD extension, absence of MT	100
Emx2	KO	Regression of whole WD	11
Wnt9b	KO	Absence of MT, absence of epididymis	17
Fgf8	*T-Cre*	Regression of cranial mesonephros	13
Fgfr1/2	*T-Cre*	Dysgenesis of WD and MT	13
	Pax3-Cre	Absence of MT	15
Fgfr2	*Hoxb7-Cre*	Regression of caudal WD	16
Shh	KO	Numerous ectopic MT, ectopic UB	29
Foxc1/2	*Foxc1/Mf1^{ch}*, KO	Numerous ectopic MT, ectopic UB	28, 101
c-ret	*ret-k^{-}*	Reduced number of MT	102
Raldh2	KO	Absence of WD	103
Lfng	KO	Blockage of the connection between efferent duct and rete testis	36
Defects in WD stabilization, elongation and coiling			
Ar	*Tfm*, KO	WD regression	40,41
Inhba	KO	Failed to develop ductal coiling in epididymis	53
Sfrp1/2	dKO	Shortened vas deferens	56
Vagl2	*Vangl2$^{lp/lp}$*	Shortened vas deferens	56
Wnt5a	KO	Shortened vas deferens	56
Pkd1	KO, *Pax2-Cre*	Coiling defect, cystic dilation of efferent ducts	54
Defects in postnatal differentiation			
Pten	*Rnase10-Cre*	Dedifferentiation of IS	2
Ros1	KO	Undifferentiated IS	1
Dusp6	KO	Large caput and corpus	67
Frs2	*Hoxb7-Cre*	Morphologically normal	68
	Rnase10-Cre	Abnormal shape of epididymis	68
Ar	*Ap2a-Cre*	Defective epithelial cell differentiation	47
	Rnase10-Cre	Absence of IS, defective epithelial cell differentiation	70
	FoxG-Cre	Absence of IS, defective epithelial cell differentiation	71
	Probasin-Cre	Small epididymis and seminal vesicle	69
Dicer	*Defb4-Cre*	Epithelial cell dedifferentiation	75
miR-29a	*miR-29b1^{UBC}* transgene	Hypoplastic epididymis	77
Lgr4	*Lgr4$^{Gt/Gt}$*	Short, dilated and much less convoluted epididymal ducts	104
	KO	Blockage of efferent duct	105
Shp1	*mev/mev*	Aberrant epididymal region	66
Hoxa11	KO	Transformation of vas deferens to epididymis	79
Hoxa10	KO	Transformation of vas deferens to epididymis	80

WD: wolffian duct; MT: mesonephric tubules; UB: ureteric bud; IS: initial segment; MD: mullerian duct

network of ductules is formed by simple fusion of a subset of MTs. The latter hypothesis would seem more feasible than the first because of the presence of blind-ended tubules. These MTs only fuse to one other MT, leaving one end sealed, hence becoming blind-ended. Obviously, there must be considerable coordination between the fusion events that limit the number of MTs that can fuse[4,5] resulting in the conus (2–3 fused MTs) and the single common ductule.[22] Identification of the genes and processes by which the formation and patterning of the efferent ducts occur is crucial, and the GUDMAP *in situ* hybridization database (http://www.gudmap.org/index.html)[31,32] clearly shows some potential genes that may regulate their formation, e.g., collagen triple helix repeat containing 1*(Cthrc1)*, cortexin 3 *(Ctxn3)* and laminin, alpha1 *(Lama1)*. *Lunatic fringe* (*Lfng*) is one of the mammalian *fringe* genes encoding a modifier of the notch receptor expressed in the developing WD, MTs and testis.[33–35] *Lfng*-null mice show partial bilateral blockage of the connection between the rete testis and the efferent ducts, indicating the involvement of notch signaling in establishing the rete testis-efferent duct boundary.[36]

The origins of nephron progenitor cells are suggested to differ between mesonephros and metanephros.[37] Metanephric mesenchyme is

derived from a posterior immature caudal population, which is positive for *Brachyury* (*T*) expression, and persists in the posterior end of the embryo until body axis extension is complete (**Figure 1a**). On the other hand, the WD and at least part of the mesonephric mesenchyme arise from the anterior intermediate mesoderm, which is defined by *Osr1* expression at E9.5 (**Figure 1b**). These recent studies may indicate that abnormal body axis extension affects the intermediate mesodermal cell fate. It is possible that disruption of the A-P body axis extension affects not only the metanephric mesenchyme but also the mesonephric mesenchymal distribution, and subsequently further male reproductive tract development. Conditionally-induced mutations of the planar cell polarity (PCP) pathway-related genes, *Wnt5a*, *Ror2* and *Vangl2*, which are important for A-P body axis extension, demonstrate that insufficient A-P axis extension of the posterior intermediate mesoderm is correlated with urogenital tract abnormalities.[38] It is clear that more studies are needed to examine the early formation of the intermediate mesoderm and how this translates into development of the WD.

Stabilization of the ductal system and further growth: elongation and coiling

During embryogenesis, the mesonephros gives rise to a stable male reproductive tract whereas the mesonephros in the female regresses (**Figure 1d** and **1e**). Androgens produced in the testis are a major factor regulating this stabilization.[39–42] Following gonadal sex differentiation, the testis begins to produce the androgen, testosterone, at approximately E12.5.[43,44] Unlike for other androgen-dependent organs, such as the prostate and seminal vesicle, it has been suggested that locally-produced, and not systemic androgen, from the testis is necessary for WD stabilization.[45] Indeed, fluorescence labeling of an androgen ligand shows that androgen is transported within the luminal fluid.[30] However, there are studies showing that testicular androgen delivered via the systemic circulation is sufficient to prevent WD regression. Subcutaneous testicular grafts stabilize the WD in female marsupial embryos.[46] Androgens act through the androgen receptor (AR), a member of the nuclear receptor superfamily. The expression of AR is mainly detected in the mesenchyme surrounding WD epithelia at E13.5 in the mouse. Tissue-specific *Ar* knockout (KO) analyses demonstrate that WD stabilization and coiling is induced in the absence of epithelial-expressed *Ar*, demonstrating the importance of *Ar* in the mesenchyme.[47] This finding is consistent with the observation from tissue recombination experiments on androgen-insensitive *Testicular feminized* (*Tfm*) mice.[48,49] Several growth factors, including FGF and Epidermal growth factor (EGF), are suggested to mediate androgen functions in the prostate and WD.[50–52] However, the molecular mechanisms by which androgens regulate these genes *in vivo* are not known.

To create a long, highly-convoluted epididymal duct, the WD begins to elongate and coil from E15.5, following stabilization (**Figure 1e**). This process is also androgen-dependent, but growth factor signaling has been reported to regulate this elongation event. Tomaszewski *et al.* reported that *Inhba*, a subunit of both inhibins and activins, is a regional paracrine factor in mouse mesonephroi that controls coiling of the epithelium in the anterior WD.[53] *Pkd1*, whose mutation accounts for 85% of autosomal dominant polycystic kidney disease, and is a membrane-spanning glycoprotein involved in growth factor signaling transduction and cytoskeleton dynamics. Epithelial coiling is absent from the *Pkd1* mutant.[54] In both mutations, epithelial cell proliferation is attenuated. Recently, mathematical modeling has suggested that epididymal tubule morphogenesis is dependent upon the cell proliferation area in the tubule and mechanical resistance from the tissues surrounding the tubule.[55]

The secreted frizzled-related proteins (SFRPs) antagonize WNT ligand protein binding to its receptor FZD. The double KO (dKO) of *Sfrp1* and *Sfrp2* genes results in a shortened WD and vas deferens.[56] Androgen administration to these animals never rescues this phenotype, indicating that the abnormalities in *Sfrp1/2* dKO mutant male embryos are not caused by insufficient production of testosterone from the testes, but may reflect insensitivity of some target tissues to androgens.[56] It is also possible to consider that these phenotypes are, at least partially, a secondary consequence of the A-P extension defect of intermediate mesoderm formation described above. Although recent analyses have partially revealed the molecular mechanisms of ductal morphogenesis, further analyses should be performed including how androgen signaling regulates these molecules.

Postnatal differentiation: regional differentiation and epithelial cell differentiation

The epididymis consists of distinct anatomical regions that vary between species. However, in the mouse four regions can be defined: initial segment and caput, corpus and cauda epididymidis (**Figure 1f**). Each region is further divided into many segments characterized by expression of specific mRNAs, proteins and a repertoire of cell types.[57,58] The segments, divided by septa, are observed after birth and are distinct during puberty, postnatal (P) days 14–35. Impaired epididymal regionalization or epithelial cell differentiation results in male infertility. For example, if the initial segment does not develop, then male infertility results. Data from efferent duct ligation (EDL) experiments suggested that luminal fluid coming from testis is responsible for the maintenance of initial segment cell survival, proliferation and differentiation.[59,60]

Several growth factors, including FGFs 2,4 and 8, are detected in testicular fluid, and *Fgfrs* are expressed in the epithelium of the initial segment.[61,62] During normal development, high activity of the MAPK pathway, especially p-MAPK1/3 (p-ERK1/2), is detected in the initial segment.[60] EDL abolishes their activities, emphasizing the importance of lumicrine factors regulating their activity.[60] *Ros1* encodes an orphan receptor tyrosine kinase that is expressed in few epithelia, among them the WD and its derivatives.[63–65] Loss of *Ros1* expression or a naturally-occurring mutation of *Shp1* (*me*^{v}), a negative regulator of ROS1, results in abnormal differentiation of the initial segment.[1,66] *RNase10-Cre* drives gene recombination in the initial segment epithelia from P17 onward. *RNase-Cre*-mediated mutation in *Pten*, a negative regulator of PIP3/AKT signaling, induces dedifferentiation of the initial segment.[2] In these animals, abnormal differentiation results in an abnormally shaped initial segment. MAPK signaling regulators such as DUSP6 and FRS2 play important roles in epididymal cell proliferation and survival during postnatal development.[67,68]

Androgens are important regulators of epididymal development from embryonic to adult stages. From later stages of development to the adult stage, *Ar* expression in the epithelia is greater than that in the mesenchyme. Several *Ar* KO mice have been reported, and the majority show a hypoplastic epididymis and defective epithelial cell differentiation.[47,69–71] A differentiated epididymal epithelium is pseudostratified and comprises principal, clear, narrow, basal and recently-identified dendritic cells throughout the duct.[72,73] Similar to other pseudostratified epithelia, for example the trachea, the epididymal luminal environment regulates secretion and absorption of ions, water, organic solutes and proteins.[74] The molecular mechanisms of epididymal epithelial differentiation are not clear. Chimeric mutation of the *Ar* indicates that defective epithelial cell differentiation is cell-autonomous.[47] Dicer and small RNAs also regulate epididymal

development and epithelial cell differentiation partially through androgen action.[75–77]

Hox genes are evolutionarily-conserved transcriptional regulators that determine body patterning.[78] As found for body plan formation, vertebrae and the gut, *Hox* genes, *Hoxa10* and *Hoxa11* are suggested to determine the boundary between the epididymis and vas deferens.[79–81] Later studies by Snyder *et al.*[82] showed that there were additional region-specific (efferent ducts, epididymis and vas deferens) *Hox* transcripts that may define boundaries along the reproductive tract during development.

POSSIBLE CONTRIBUTION OF MOUSE MODELS TO UNDERSTAND HUMAN CINICAL ABNORMALITIES

One of the most well-known congenital anomalies of the epididymis or vas deferens is congenital bilateral absence of the vas deferens (CBAVD). It occurs in 1%–2% of men with infertility.[83] 60%–90% of the CBAVD men harbor at least one associated *cystic fibrosis transmembrane conductance regulator* (*CFTR*) gene mutation.[84] 10%–40% of CBAVD men do not have recognizable *CFTR* gene abnormalities accompanied by unilateral renal agenesis (URA).[85] Presumably, CBAVD patients have disrupted morphogenesis of the early mesonephros owing to the mutation of genes.[86] Those genes involved in mesonephros formation, e.g., *Pax2*, *Wt-1* and *Fgfs*, may be viable candidate genes responsible for CBAVD with renal malformation.

Conversely, congenital anomalies of kidney and urinary tract (CAKUT) often carry mutations in genes, such as *PAX2* and *WT-1*, and male mice carrying mutations of these genes also exhibit reproductive tract malformations.[87] Syndromes with renal tract abnormalities also carry mutations in the genes described above. Branchio-Oto-Renal (BOR) syndrome is a genetic condition that typically disrupts the development of tissues in the neck and causes malformations of the ears and kidneys. *EYA1*, the human homolog of the *Drosophila eyes absent* gene, is the most common gene responsible for BOR.[88] Further, *Foxc1* regulates *Eya1* expression.[28] Mutations in the *SIX1* gene can be detected in 2% of individuals with the clinical diagnosis of BOR.[89] Mutations in both *ROR2*[90] and *WNT5A*[91] have been implicated in a rare genetic disease, Robinow syndrome, which exhibits several defects such as dwarfism, hydronephrosis and genital abnormalities. Because these syndromes often exhibit lethal abnormalities, it is still unclear if these mutations affect male fertility in humans.

Epididymal disjunction is the failure of the efferent ducts to reach the testis, which may reflect the failure of the efferent ducts to elongate, and presumably coil, during their development.[92–95] Interestingly, one study[95] has shown that 30%–79% of boys with an undescended testis also have Wolffian duct abnormalities, of which 25% display epididymal disjunction. Therefore, it is important that epididymal abnormalities be detected at orchidopexy, or other male infertility, which may be classified as idiopathic, will result. As mentioned above, it is not clear how the efferent ducts form, elongate, are directed toward the testis and then fuse with the rete testis. Obviously, mouse models that display epididymal disjunction will greatly aid our understanding of this abnormality.

SUMMARY

One of the striking characteristics of the epididymis is its complex developmental process. The primordium of the epididymis, the mesonephros, arises as a part of the transient kidney, and its stability and differentiation are regulated by hormonal signaling including by androgens and growth factors. In human, it transforms its morphology to form a 6 m duct that is coiled and packed into a three-dimensional organ of approximately 10 cm in length. Recent studies utilizing a variety of transgenic mice have revealed the molecular contribution of numerous factors at each stage of epididymal development. The molecular dissection of the developmental mechanisms of the epididymis has just begun. Integrative understanding of the hierarchy and interaction of each factor will provide new directions in this field. Considering that the epididymis shares its origin with the urinary tract, it is noteworthy that the molecular mechanisms which lead to kidney mal-development, such as CAKUT, may provide significant insight for the mesonephros derivative mal-development, such as CBAVD and *vice versa*.

COMPETING FINANCIAL INTERESTS

Neither author declares a competing interest.

ACKNOWLEDGMENTS

We would like to thank Prof. Gen Yamada and Dr. Mika Okazawa for the supportive discussion. This work is supported by Grant-in-Aid for Young Scientists B (25860771), and National Institutes of Health Eunice Kennedy Shriver NICHD Grants HD069654 and HD068365 (BTH).

REFERENCES

1 Sonnenberg-Riethmacher E, Walter B, Riethmacher D, Gödecke S, Birchmeier C. The c-ros tyrosine kinase receptor controls regionalization and differentiation of epithelial cells in the epididymis. *Genes Dev* 1996; 10: 1184–93.
2 Xu B, Washington AM, Hinton BT. PTEN signaling through RAF1 proto-oncogene serine/threonine kinase (RAF1)/ERK in the epididymis is essential for male fertility. *Proc Natl Acad Sci U S A* 2014; 111: 18643–8.
3 Yeung CH, Cooper TG, Bergmann M, Schulze H. Organization of tubules in the human caput epididymidis and the ultrastructure of their epithelia. *Am J Anat* 1991; 191: 261–79.
4 Atsuta Y, Tadokoro R, Saito D, Takahashi Y. Transgenesis of the Wolffian duct visualizes dynamic behavior of cells undergoing tubulogenesis *in vivo*. *Dev Growth Differ* 2013; 55: 579–90.
5 Staack A, Donjacour AA, Brody J, Cunha GR, Carroll P. Mouse urogenital development: a practical approach. *Differentiation* 2003; 71: 402–13.
6 Saxen, L. Organogenesis of the Kidney. Cambridge University Press; 1987.
7 Torres M, Gómez-Pardo E, Dressler GR, Gruss P. Pax-2 controls multiple steps of urogenital development. *Development* 1995; 121: 4057–65.
8 Bouchard M, Souabni A, Mandler M, Neubüser A, Busslinger M. Nephric lineage specification by Pax2 and Pax8. *Genes Dev* 2002; 16: 2958–70.
9 Pedersen A, Skjong C, Shawlot W. Lim 1 is required for nephric duct extension and ureteric bud morphogenesis. *Dev Biol* 2005; 288: 571–81.
10 Kobayashi A, Shawlot W, Kania A, Behringer RR. Requirement of Lim1 for female reproductive tract development. *Development* 2004; 131: 539–49.
11 Miyamoto N, Yoshida M, Kuratani S, Matsuo I, Aizawa S. Defects of urogenital development in mice lacking Emx2. *Development* 1997; 124: 1653–64.
12 Grote D, Souabni A, Busslinger M, Bouchard M. Pax2/8-regulated Gata 3 expression is necessary for morphogenesis and guidance of the nephric duct in the developing kidney. *Development* 2006; 133: 53–61.
13 Kitagaki J, Ueda Y, Chi X, Sharma N, Elder CM, *et al.* FGF8 is essential for formation of the ductal system in the male reproductive tract. *Development* 2011; 138: 5369–78.
14 Ornitz DM, Itoh N. Fibroblast growth factors. Genome Biol. 2001;2(3):REVIEWS3005. Epub 2001 Mar 9. Review.
15 Poladia DP, Kish K, Kutay B, Hains D, Kegg H, *et al.* Role of fibroblast growth factor receptors 1 and 2 in the metanephric mesenchyme. *Dev Biol* 2006; 291: 325–39.
16 Okazawa M, Murashima A, Harada M, Nakagata N, Noguchi M, *et al.* Region-specific regulation of cell proliferation by FGF receptor signaling during the Wolffian duct development. *Dev Biol* 2015; 400: 139–47.
17 Carroll TJ, Park JS, Hayashi S, Majumdar A, McMahon AP. Wnt9b plays a central role in the regulation of mesenchymal to epithelial transitions underlying organogenesis of the mammalian urogenital system. *Dev Cell* 2005; 9: 283–92.
18 Karner CM, Chirumamilla R, Aoki S, Igarashi P, Wallingford JB, *et al.* Wnt9b signaling regulates planar cell polarity and kidney tubule morphogenesis. *Nat Genet* 2009; 41: 793–9.
19 de Martino C, Zamboni L. A morphologic study of the mesonephros of the human embryo. *J Ultrastruct Res* 1966; 16: 399–427.
20 Tiedemann K, Egerer G. Vascularization and glomerular ultrastructure in the pig mesonephros. *Cell Tissue Res* 1984; 238: 165–75.
21 Smith C, Mackay S. Morphological development and fate of the mouse mesonephros. *J Anat* 1991; 174: 171–84.

22 Guttroff RF, Cooke PS, Hess RA. Blind-ending tubules and branching patterns of the rat ductuli efferentes. *Anat Rec* 1992; 232: 423–31.
23 Ilio KY, Hess RA. Structure and function of the ductuli efferentes: a review. *Microsc Res Tech* 1994; 29: 432–67.
24 Mansouri A, Chowdhury K, Gruss P. Follicular cells of the thyroid gland require Pax8 gene function. *Nat Genet* 1998; 19: 87–90.
25 Kreidberg JA, Sariola H, Loring JM, Maeda M, Pelletier J, *et al.* WT-1 is required for early kidney development. *Cell* 1993; 74: 679–91.
26 Sainio K, Hellstedt P, Kreidberg JA, Saxén L, Sariola H. Differential regulation of two sets of mesonephric tubules by WT-1. *Development* 1997; 124: 1293–9.
27 Kobayashi H, Kawakami K, Asashima M, Nishinakamura R. Six1 and Six4 are essential for Gdnf expression in the metanephric mesenchyme and ureteric bud formation, while Six1 deficiency alone causes mesonephric-tubule defects. *Mech Dev* 2007; 124: 290–303.
28 Kume T, Deng K, Hogan BL. Murine forkhead/winged helix genes Foxc1 (Mf1) and Foxc2 (Mfh1) are required for the early organogenesis of the kidney and urinary tract. *Development* 2000; 127: 1387–95.
29 Murashima A, Akita H, Okazawa M, Kishigami S, Nakagata N, *et al.* Midline-derived Shh regulates mesonephric tubule formation through the paraxial mesoderm. *Dev Biol* 2014; 386: 216–26.
30 Tong SY, Hutson JM, Watts LM. Does testosterone diffuse down the Wolffian duct during sexual differentiation? *J Urol* 1996; 155: 2057–9.
31 Harding SD, Armit C, Armstrong J, Brennan J, Cheng Y, *et al.* The GUDMAP database – an online resource for genitourinary research. *Development* 2011; 138: 2845–53.
32 McMahon AP, Aronow BJ, Davidson DR, Davies JA, Gaido KW, *et al.* GUDMAP: the genitourinary developmental molecular anatomy project. *J Am Soc Nephrol* 2008; 19: 667–71.
33 Johnston SH, Rauskolb C, Wilson R, Prabhakaran B, Irvine KD, *et al.* A family of mammalian Fringe genes implicated in boundary determination and the Notch pathway. *Development* 1997; 124: 2245–54.
34 Lupien M, Diévart A, Morales CR, Hermo L, Calvo E, *et al.* Expression of constitutively active Notch1 in male genital tracts results in ectopic growth and blockage of efferent ducts, epididymal hyperplasia and sterility. *Dev Biol* 2006; 300: 497–511.
35 Evrard YA, Lun Y, Aulehla A, Gan L, Johnson RL. Lunatic fringe is an essential mediator of somite segmentation and patterning. *Nature* 1998; 394: 377–81.
36 Hahn KL, Beres B, Rowton MJ, Skinner MK, Chang Y, *et al.* A deficiency of lunatic fringe is associated with cystic dilation of the rete testis. *Reproduction* 2009; 137: 79–93.
37 Taguchi A, Kaku Y, Ohmori T, Sharmin S, Ogawa M, *et al.* Redefining the *in vivo* origin of metanephric nephron progenitors enables generation of complex kidney structures from pluripotent stem cells. *Cell Stem Cell* 2014; 14: 53–67.
38 Yun K, Ajima R, Sharma N, Costantini F, Mackem S, *et al.* Non-canonical Wnt5a/Ror2 signaling regulates kidney morphogenesis by controlling intermediate mesoderm extension. *Hum Mol Genet* 2014; 23: 6807–14.
39 Jost A. Recherches sur la différenciation sexuelle de l'embryon de Lapin. *Arch Anat Microsc Morphol Exp* 1947; 36: 151–315.
40 Lyon MF, Hawkes SG. X-linked gene for testicular feminization in the mouse. *Nature* 1970; 227: 1217–9.
41 Matsumoto T, Takeyama K, Sato T, Kato S. Androgen receptor functions from reverse genetic models. *J Steroid Biochem Mol Biol* 2003; 85: 95–9.
42 Welsh M, Sharpe RM, Walker M, Smith LB, Saunders PT. New insights into the role of androgens in Wolffian duct stabilization in male and female rodents. *Endocrinology* 2009; 150: 2472–80.
43 Shima Y, Miyabayashi K, Haraguchi S, Arakawa T, Otake H, *et al.* Contribution of Leydig and Sertoli cells to testosterone production in mouse fetal testes. *Mol Endocrinol* 2013; 27: 63–73.
44 DeFalco T, Capel B. Gonad morphogenesis in vertebrates: divergent means to a convergent end. *Annu Rev Cell Dev Biol* 2009; 25: 457–82.
45 Jost A. Problems of fetal endocrinology: the gonadal and hypophyseal hormones. *Recent Prog Horm Res* 1953; 8: 379–418.
46 Renfree MB, Fenelon J, Wijiyanti G, Wilson JD, Shaw G. Wolffian duct differentiation by physiological concentrations of androgen delivered systemically. *Dev Biol* 2009; 334: 429–36.
47 Murashima A, Miyagawa S, Ogino Y, Nishida-Fukuda H, Araki K, *et al.* Essential roles of androgen signaling in Wolffian duct stabilization and epididymal cell differentiation. *Endocrinology* 2011; 152: 1640–51.
48 Cunha GR, Young P, Higgins SJ, Cooke PS. Neonatal seminal vesicle mesenchyme induces a new morphological and functional phenotype in the epithelia of adult ureter and ductus deferens. *Development* 1991; 111: 145–58.
49 Cunha GR, Alarid ET, Turner T, Donjacour AA, Boutin EL, *et al.* Normal and abnormal development of the male urogenital tract. Role of androgens, mesenchymal-epithelial interactions, and growth factors. *J Androl* 1992; 13: 465–75.
50 Donjacour AA, Thomson AA, Cunha GR. FGF-10 plays an essential role in the growth of the fetal prostate. *Dev Biol* 2003; 261: 39–54.
51 Gupta C. The role of epidermal growth factor receptor (EGFR) in male reproductive tract differentiation: stimulation of EGFR expression and inhibition of Wolffian duct differentiation with anti-EGFR antibody. *Endocrinology* 1996; 137: 905–10.
52 Gupta C, Siegel S, Ellis D. The role of EGF in testosterone-induced reproductive tract differentiation. *Dev Biol* 1991; 146: 106–16.
53 Tomaszewski J, Joseph A, Archambeault D, Yao HH. Essential roles of inhibin beta A in mouse epididymal coiling. *Proc Natl Acad Sci U S A* 2007; 104: 11322–7.
54 Nie X, Arend LJ. Pkd1 is required for male reproductive tract development. *Mech Dev* 2013; 130: 567–76.
55 Hirashima T. Pattern formation of an epithelial tubule by mechanical instability during epididymal development. *Cell Rep* 2014; 9: 866–73.
56 Warr N, Siggers P, Bogani D, Brixey R, Pastorelli L, *et al.* Sfrp1 and Sfrp2 are required for normal male sexual development in mice. *Dev Biol* 2009; 326: 273–84.
57 Johnston DS, Jelinsky SA, Bang HJ, DiCandeloro P, Wilson E, *et al.* The mouse epididymal transcriptome: transcriptional profiling of segmental gene expression in the epididymis. *Biol Reprod* 2005; 73: 404–13.
58 Abou-Haïla A, Fain-Maurel MA. Regional differences of the proximal part of mouse epididymis: morphological and histochemical characterization. *Anat Rec* 1984; 209: 197–208.
59 Turner TT, Riley TA. p53 independent, region-specific epithelial apoptosis is induced in the rat epididymis by deprivation of luminal factors. *Mol Reprod Dev* 1999; 53: 188–97.
60 Xu B, Abdel-Fattah R, Yang L, Crenshaw SA, Black MB, *et al.* Testicular lumicrine factors regulate ERK, STAT, and NFKB pathways in the initial segment of the rat epididymis to prevent apoptosis. *Biol Reprod* 2011; 84: 1282–91.
61 Lan ZJ, Labus JC, Hinton BT. Regulation of gamma-glutamyl transpeptidase catalytic activity and protein level in the initial segment of the rat epididymis by testicular factors: role of basic fibroblast growth factor. *Biol Reprod* 1998; 58: 197–206.
62 Kirby JL, Yang L, Labus JC, Hinton BT. Characterization of fibroblast growth factor receptors expressed in principal cells in the initial segment of the rat epididymis. *Biol Reprod* 2003; 68: 2314–21.
63 Sonnenberg E, Gödecke A, Walter B, Bladt F, Birchmeier C. Transient and locally restricted expression of the ros1 protooncogene during mouse development. *EMBO J* 1991; 10: 3693–702.
64 Tessarollo L, Nagarajan L, Parada LF. c-ros: the vertebrate homolog of the sevenless tyrosine kinase receptor is tightly regulated during organogenesis in mouse embryonic development. *Development* 1992; 115: 11–20.
65 Chen J, Zong CS, Wang LH. Tissue and epithelial cell-specific expression of chicken proto-oncogene c-ros in several organs suggests that it may play roles in their development and mature functions. *Oncogene* 1994; 9: 773–80.
66 Keilhack H, Müller M, Böhmer SA, Frank C, Weidner KM, *et al.* Negative regulation of Ros receptor tyrosine kinase signaling. An epithelial function of the SH2 domain protein tyrosine phosphatase SHP-1. *J Cell Biol* 2001; 152: 325–34.
67 Xu B, Yang L, Lye RJ, Hinton BT. p-MAPK1/3 and DUSP6 regulate epididymal cell proliferation and survival in a region-specific manner in mice. *Biol Reprod* 2010; 83: 807–17.
68 Xu B, Yang L, Hinton BT. The role of fibroblast growth factor receptor substrate 2 (FRS2) in the regulation of two activity levels of the components of the extracellular signal-regulated kinase (ERK) pathway in the mouse epididymis. *Biol Reprod* 2013; 89: 1–13.
69 Simanainen U, McNamara K, Davey RA, Zajac JD, Handelsman DJ. Severe subfertility in mice with androgen receptor inactivation in sex accessory organs but not in testis. *Endocrinology* 2008; 149: 3330–8.
70 Krutskikh A, De Gendt K, Sharp V, Verhoeven G, Poutanen M, *et al.* Targeted inactivation of the androgen receptor gene in murine proximal epididymis causes epithelial hypotrophy and obstructive azoospermia. *Endocrinology* 2011; 152: 689–96.
71 O'Hara L, Welsh M, Saunders PT, Smith LB. Androgen receptor expression in the caput epididymal epithelium is essential for development of the initial segment and epididymal spermatozoa transit. *Endocrinology* 2011; 152: 718–29.
72 Sun EL, Flickinger CJ. Development of cell types and of regional differences in the postnatal rat epididymis. *Am J Anat* 1979; 154: 27–55.
73 Da Silva N, Cortez-Retamozo V, Reinecker HC, Wildgruber M, Hill E, *et al.* A dense network of dendritic cells populates the murine epididymis. *Reproduction* 2011; 141: 653–63.
74 Shum WW, Da Silva N, McKee M, Smith PJ, Brown D, *et al.* Transepithelial projections from basal cells are luminal sensors in pseudostratified epithelia. *Cell* 2008; 135: 1108–17.
75 Björkgren I, Saastamoinen L, Krutskikh A, Huhtaniemi I, Poutanen M, *et al.* Dicer1 ablation in the mouse epididymis causes dedifferentiation of the epithelium and imbalance in sex steroid signaling. *PLoS One* 2012; 7: e38457.
76 Ma W, Xie S, Ni M, Huang X, Hu S, *et al.* MicroRNA-29a inhibited epididymal epithelial cell proliferation by targeting nuclear autoantigenic sperm protein (NASP). *J Biol Chem* 2012; 287: 10189–99.
77 Ma W, Hu S, Yao G, Xie S, Ni M, *et al.* An androgen receptor-microrna-29a regulatory circuitry in mouse epididymis. *J Biol Chem* 2013; 288: 29369–81.
78 McGinnis W, Krumlauf R. Homeobox genes and axial patterning. *Cell* 1992; 68: 283–302.
79 Hsieh-Li HM, Witte DP, Weinstein M, Branford W, Li H, *et al.* Hoxa 11 structure, extensive antisense transcription, and function in male and female fertility. *Development* 1995; 121: 1373–85.

80 Podlasek CA, Seo RM, Clemens JQ, Ma L, Maas RL, *et al.* Hoxa-10 deficient male mice exhibit abnormal development of the accessory sex organs. *Dev Dyn* 1999; 214: 1–12.
81 Bomgardner D, Hinton BT, Turner TT. Hox transcription factors may play a role in regulating segmental function of the adult epididymis. *J Androl* 2001; 22: 527–31.
82 Snyder EM, Small CL, Bomgardner D, Xu B, Evanoff R, *et al.* Gene expression in the efferent ducts, epididymis, and vas deferens during embryonic development of the mouse. *Dev Dyn* 2010; 239: 2479–91.
83 Jequier AM, Ansell ID, Bullimore NJ. Congenital absence of the vasa deferentia presenting with infertility. *J Androl* 1985; 6: 15–9.
84 Anguiano A, Oates RD, Amos JA, Dean M, Gerrard B, *et al.* Congenital bilateral absence of the vas deferens. A primarily genital form of cystic fibrosis. *JAMA* 1992; 267: 1794–7.
85 Augarten A, Yahav Y, Kerem BS, Halle D, Laufer J, *et al.* Congenital bilateral absence of vas deferens in the absence of cystic fibrosis. *Lancet* 1994; 344: 1473–4.
86 McCallum T, Milunsky J, Munarriz R, Carson R, Sadeghi-Nejad H, *et al.* Unilateral renal agenesis associated with congenital bilateral absence of the vas deferens: phenotypic findings and genetic considerations. *Hum Reprod* 2001; 16: 282–8.
87 Pope JC 4th, Brock JW 3rd, Adams MC, Stephens FD, Ichikawa I. How they begin and how they end: classic and new theories for the development and deterioration of congenital anomalies of the kidney and urinary tract, CAKUT. *J Am Soc Nephrol* 1999; 10: 2018–28.
88 Abdelhak S, Kalatzis V, Heilig R, Compain S, Samson D, *et al.* A human homologue of the *Drosophila* eyes absent gene underlies branchio-oto-renal (BOR) syndrome and identifies a novel gene family. *Nat Genet* 1997; 15: 157–64.
89 Kochhar A, Orten DJ, Sorensen JL, Fischer SM, Cremers CW, *et al.* SIX1 mutation screening in 247 branchio-oto-renal syndrome families: a recurrent missense mutation associated with BOR. *Hum Mutat* 2008; 29: 565.
90 Afzal AR, Rajab A, Fenske CD, Oldridge M, Elanko N, *et al.* Recessive Robinow syndrome, allelic to dominant brachydactyly type B, is caused by mutation of ROR2. *Nat Genet* 2000; 25: 419–22.
91 Person AD, Beiraghi S, Sieben CM, Hermanson S, Neumann AN, *et al.* WNT5A mutations in patients with autosomal dominant Robinow syndrome. *Dev Dyn* 2010; 239: 327–37.
92 Girgis SM, Etriby AN, Ibrahim AA, Kahil SA. Testicular biopsy in azoospermia. A review of the last ten years' experiences of over 800 cases. *Fertil Steril* 1969; 20: 467–77.
93 Kroovand RL, Perlmutter AD. Congenital anomalies of the vas deferens and epididymis. In: SJ Hogan and ESE Hafez, editors. Pediatric Andrology. Boston: Martinus Nijhoff Publishers; 1981. p. 173–80.
94 Turek PJ, Ewalt DH, Snyder HM, Duckett JW. Normal epididymal anatomy in boys. *J Urol* 1994; 151: 726–7.
95 Zvizdic Z, Huskic J, Dizdarevic S, Karavdic K, Zvizdic D. Incidence of epididymal disjunction anomalies associated with an undescended testis. *Folia Med* 2009; 44: 65–8.
96 Tzouanacou E, Wegener A, Wymeersch FJ, Wilson V, Nicolas JF. Redefining the progression of lineage segregations during mammalian embryogenesis by clonal analysis. *Dev Cell* 2009; 17: 365–76.
97 Takemoto T, Uchikawa M, Yoshida M, Bell DM, Lovell-Badge R, *et al.* Tbx6-dependent Sox2 regulation determines neural or mesodermal fate in axial stem cells. *Nature* 2011; 470: 394–8.
98 Chia I, Grote D, Marcotte M, Batourina E, Mendelsohn C, *et al.* Nephric duct insertion is a crucial step in urinary tract maturation that is regulated by a Gata3-Raldh2-Ret molecular network in mice. *Development* 2011; 138: 2089–97.
99 Pole RJ, Qi BQ, Beasley SW. Patterns of apoptosis during degeneration of the pronephros and mesonephros. *J Urol* 2002; 167: 269–71.
100 Wang Q, Lan Y, Cho ES, Maltby KM, Jiang R. Odd-skipped related 1 (Odd 1) is an essential regulator of heart and urogenital development. *Dev Biol* 2005; 288: 582–94.
101 Mattiske D, Kume T, Hogan BL. The mouse forkhead gene Foxc1 is required for primordial germ cell migration and antral follicle development. *Dev Biol* 2006; 290: 447–58.
102 Schuchardt A, D'Agati V, Pachnis V, Costantini F. Renal agenesis and hypodysplasia in ret-k- mutant mice result from defects in ureteric bud development. *Development* 1996; 122: 1919–29.
103 Niederreither K, Subbarayan V, Dollé P, Chambon P. Embryonic retinoic acid synthesis is essential for early mouse post-implantation development. *Nat Genet* 1999; 21: 444–8.
104 Hoshii T, Takeo T, Nakagata N, Takeya M, Araki K, *et al.* LGR4 regulates the postnatal development and integrity of male reproductive tracts in mice. *Biol Reprod* 2007; 76: 303–13.
105 Mendive F, Laurent P, Van Schoore G, Skarnes W, Pochet R, *et al.* Defective postnatal development of the male reproductive tract in LGR4 knockout mice. *Dev Biol* 2006; 290: 421–34.

DEVELOPMENTAL BIOLOGY

Elimination of the male reproductive tract in the female embryo is promoted by COUP-TFII in mice

Fei Zhao,[1] Heather L. Franco,[1] Karina F. Rodriguez,[1] Paula R. Brown,[1] Ming-Jer Tsai,[2] Sophia Y. Tsai,[2] Humphrey H.-C. Yao[1]*

The sexual differentiation paradigm contends that the female pattern of the reproductive system is established by default because the male reproductive tracts (Wolffian ducts) in the female degenerate owing to a lack of androgen. Here, we discovered that female mouse embryos lacking *Coup-tfII* (chicken ovalbumin upstream promoter transcription factor II) in the Wolffian duct mesenchyme became intersex—possessing both female and male reproductive tracts. Retention of Wolffian ducts was not caused by ectopic androgen production or action. Instead, enhanced phosphorylated extracellular signal-regulated kinase signaling in Wolffian duct epithelium was responsible for the retention of male structures in an androgen-independent manner. We thus suggest that elimination of Wolffian ducts in female embryos is actively promoted by COUP-TFII, which suppresses a mesenchyme-epithelium cross-talk responsible for Wolffian duct maintenance.

Sexually dimorphic establishment of reproductive tracts epitomizes the anatomical difference between males and females. This dimorphic establishment depends on two concurrent events during embryogenesis: regression of one of the two primitive ducts (Müllerian and Wolffian ducts) and maintenance of the other. These two events ensure that the embryo retains only one reproductive tract that corresponds to its sex: Müllerian duct for the XX individual and Wolffian duct for the XY individual (*1*). In the 1950s, Alfred Jost provided the first evidence for what became the foundation of the sexual differentiation paradigm: XY embryos retain Wolffian ducts through the action of testis-derived androgen, whereas XX embryos lose Wolffian ducts as a result of a lack of androgens (*2*–*5*).

The action of androgen on the Wolffian duct is mediated through androgen receptors in the mesenchyme surrounding Wolffian ducts (*6*, *7*). It is well established that mesenchyme-derived factors govern the fate and differentiation of ductal epithelium (*8*). The orphan nuclear receptor COUP-TFII (chicken ovalbumin upstream promoter transcription factor II, or NR2F2) is a mesenchyme-specific regulator in many developing organs, including the mesonephros, where Wolffian ducts develop (*9*). COUP-TFII expression in Wolffian duct mesenchyme overlapped with Wilms' Tumor 1 (WT1) (fig. S1A), another mesenchyme-specific transcriptional factor (*10*). To investigate the role of COUP-TFII in Wolffian duct regression, we used the tamoxifen-inducible $Wt1^{CreERT2}$ mouse model that targeted *Coup-tfII* deletion in $Wt1^{+}$ mesenchymal cells (fig. S1B). In the control ($Wt1^{CreERT2-}$;$Coup\text{-}tfII^{f/f}$) female, COUP-TFII remained in the mesenchymal cells of mesonephroi from embryonic day 12.5 (E12.5) to E16.5 (fig. S1, C to E), the developmental window that encompassed initiation (E14.5) and completion (E16.5) of Wolffian duct regression in XX embryos (fig. 2SA). In the knockout ($Wt1^{CreERT2+}$;$Coup\text{-}tfII^{f/f}$) female, COUP-TFII ablation began 24 hours after the first tamoxifen injection (fig. S1F) and was completed by E14.5 (fig. S1, G and H). Ablation of *Coup-tfII* was further confirmed with reverse transcription polymerase chain reaction (RT-PCR) (fig. S2B). These results demonstrated an efficient ablation of *Coup-tfII* in WT1-positive Wolffian duct mesenchyme in XX embryos.

The impact of *Coup-tfII* ablation on XX mesonephroi was first examined at E18.5, when dimorphic development of reproductive tracts is completed. The control XX embryos contained only Müllerian ducts that were visualized by immunostaining of the epithelial marker PAX2 (Fig. 1A). Other control genotypes that include $Wt1^{CreERT2+}$;$Coup\text{-}tfII^{f/+}$ and $Wt1^{CreERT2+}$;$Coup\text{-}tfII^{+/+}$ female embryos also developed normally, with only Müllerian ducts (fig. S3A). Knockout XX littermates, however, had both Müllerian and Wolffian ducts in the mesonephros (Fig. 1D). The identity of the Wolffian duct was confirmed by the presence of Wolffian duct epithelium marker transcription factor AP-2α (AP-2α) (Fig. 1, B and E) (*7*). Embryos in which *Coup-tfII* was knocked out died soon after birth. We therefore developed an organ culture system that allowed us to maintain E18.5 XX mesonephros with ovaries for 7 days to investigate whether Wolffian ducts remained present postnatally. At the end of culture, Wolffian ducts were still present in knockout tissues, along with the components of female reproductive tracts (Fig. 1, C and F), indicating that Wolffian duct maintenance in knockout XX persisted after birth and was not a transient event.

Retention of Wolffian ducts in the *Coup-tfII* knockout XX embryo points to a possible action of androgens based on the Jost paradigm (*11*). $Wt1^{CreERT2}$ targets *Coup-tfII* deletion not only in mesonephroi but also somatic cells of the ovary (*12*), raising the possibility that an ovary in which *Coup-tfII* has been knocked out could synthesize androgens ectopically. We compared the transcriptomes between control and knockout ovaries at E14.5 and E16.5, during which Wolffian duct regression occurs. The transcriptome of the knockout ovary was not different from the control ovary, with the exception of 10 differentially expressed genes (including *Coup-tfII*) (table S1). None of these genes were associated with androgen production. Furthermore, mRNA expression of two rate-limiting enzymes—hydroxy-δ-5-steroid dehydrogenase, 3β- and steroid δ-isomerase 1(*Hsd3b1*) and cytochrome P450 17A1 (*Cyp17a1*)—for steroidogenesis was not different between control and knockout ovaries and nearly undetectable compared with the wild-type fetal testis (a positive control) (Fig. 2, A and B). A lack of androgen-producing capacity in the ovary was corroborated with unchanged anogenital distance (AGD), an androgen-sensitive parameter, between control and knockout XX at E18.5 (Fig. 2C). To exclude the possibility that androgens came from other resources in the knockout embryo, we removed the mesonephroi from XX embryos and cultured them for 4 days. After culture, Wolffian ducts regressed in control XX mesonephros, as expected, whereas in knockout XX, either in the presence or absence of ovaries, Wolffian ducts were maintained (Fig. 2D and fig. S3B). These results indicated a lack of androgen production in the XX knockout ovaries and led us to speculate that Wolffian duct retention in XX embryos could be the result of ectopic activation of the androgen pathway in the absence of *Coup-tfII*. This possibility was excluded based on of the finding that expression of androgen receptor (*Ar*) and two androgen-induced genes—folate hydrolase 1 (*Folh1*) and solute carrier family 26 member 3 (*Slc26a3*) (*13*, *14*)—was not different between control and knockout XX mesonephroi (Fig. 2, E to G). To rule out the involvement of androgens, we exposed the dam that carried control and knockout embryos to the androgen antagonist flutamide (Fig. 2H) (*15*). This regimen was sufficient to prevent Wolffian duct maintenance resulting from ectopic androgen action in XX embryos (*16*). Despite the verified action of flutamide (fig. S4), Wolffian ducts were still retained in knockout XX embryos (Fig. 2H). Thus, the maintenance of Wolffian ducts in the *Coup-tfII* knockout XX embryo is not due to ectopic production or action of androgens.

To identify the androgen-independent mechanism underlying Wolffian duct retention in the female in which *Coup-tfII* had been knocked out, we turned our attention to epidermal growth factor (EGF) and fibroblast growth factor (FGF) signaling pathways for their putative ability to promote Wolffian duct maintenance (*17*, *18*). We first examined by means of RT-PCR the expression of *Egf* and its receptor *Egfr*. Their expression

[1]Reproductive Developmental Biology Group, National Institute of Environmental Health Sciences, Durham, NC 27709, USA. [2]Department of Molecular and Cellular Biology, Baylor College of Medicine, Houston, TX 77030, USA.
*Corresponding author. Email: humphrey.yao@nih.gov

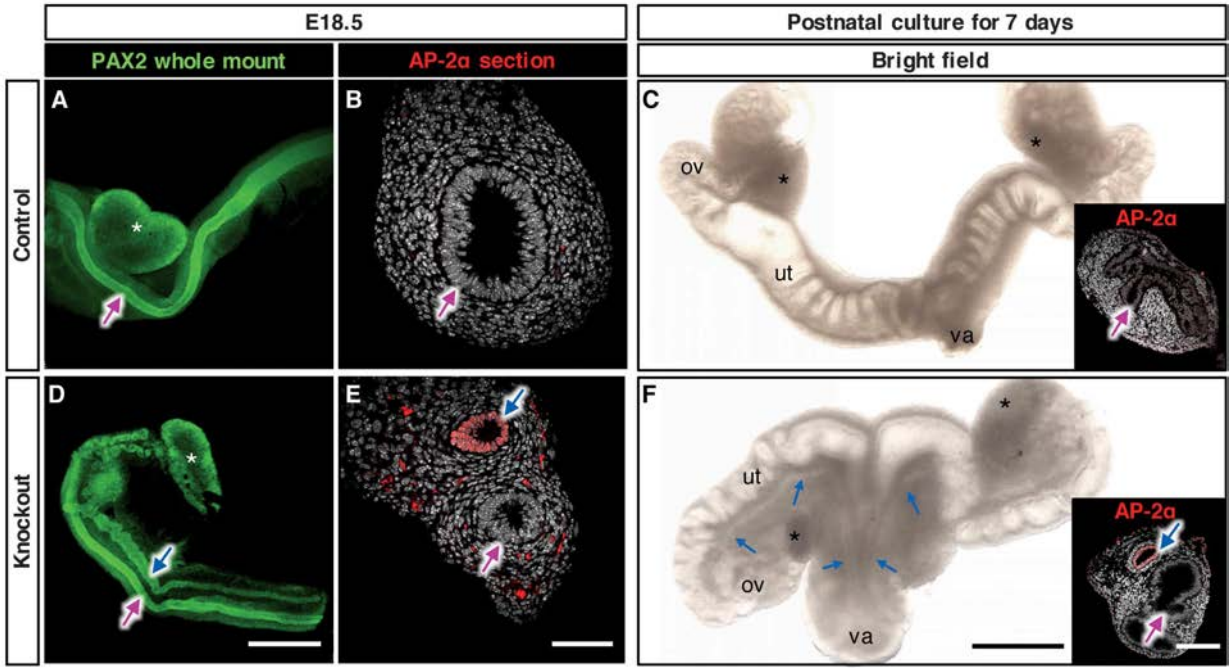

Fig. 1. *Coup-tfII* ablation leads to Wolffian duct retention in the XX embryo. Control and *Coup-tfII* knockout reproductive systems from E18.5 XX embryos were analyzed with (**A** and **D**) whole-mount immunofluorescence for the epithelial marker PAX2 or (**B** and **E**) AP-2α on frozen sections. (**C** and **F**) Control and knockout mesonephroi from E18.5 XX embryos were cultured for 7 days and analyzed with bright field microscopy or (insets) AP-2α immunofluorescence on frozen sections. Blue arrows indicate Wolffian ducts, magenta arrows indicate Müllerian ducts, and asterisks indicate ovary. ov, oviduct; ut, uterus; va, vagina. Scales bars, (A), (C), (D), (F), 0.5 mm; (B), (C) inset, (E), and (F) inset, 50 μm. n = 14 embryos in (A); n = 3 embryos per each genotype in (B), (C), (E), (F), and n = 23 embryos in (D).

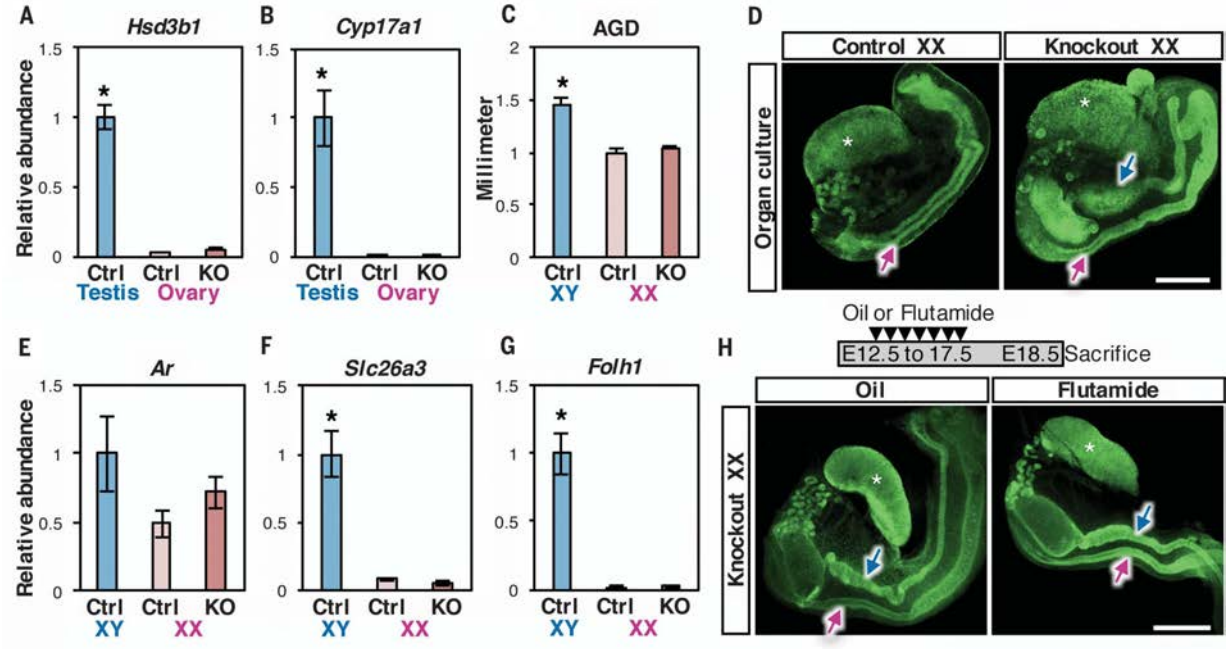

Fig. 2. Wolffian duct retention in *Coup-tfII* knockout XX embryo is independent of androgen production or action. (**A** and **B**) mRNA expression of two rate-limiting steroidogenic enzymes, *Hsd3b1* and *Cyp17a1*, in E14.5 control testis (light blue), control ovary (light pink), and knockout ovary (dark pink). (**C**) AGD of the control and knockout embryos at E18.5. (**D**) PAX2 whole-mount immunofluorescence of ovaries and mesonephroi after 4-day culture. n = 7 embryos per genotype. (**E** to **G**) mRNA expression of androgen receptor *Ar* and androgen-responsive genes (*Slc26a3* and *Folh1*) in control XY, control XX, and knockout XX mesonephroi. Results are shown as mean ± SEM. Asterisks in (A), (B), (C), (F), and (G) represent statistical significance of $P < 0.05$ compared with either control or knockout XX samples by means of one-way analysis of variance followed by Tukey's test [n = 8 embryos per each group in (A) and (B), n = 8 to 11 embryos in (C); and n = 8 embryos in (E) to (G)]. (**H**) Knockout XX embryos were exposed to either vehicle (oil) or androgen receptor antagonist flutamide in utero once daily from E12.5 to E17.5. Samples were collected at E18.5 and analyzed with PAX2 whole-mount immunofluorescence. n = 3 embryos per genotype. Blue arrows indicate Wolffian ducts, magenta arrows indicate Müllerian ducts, and white asterisk indicates ovary. Scale bar, (D) and (H), 0.5 mm.

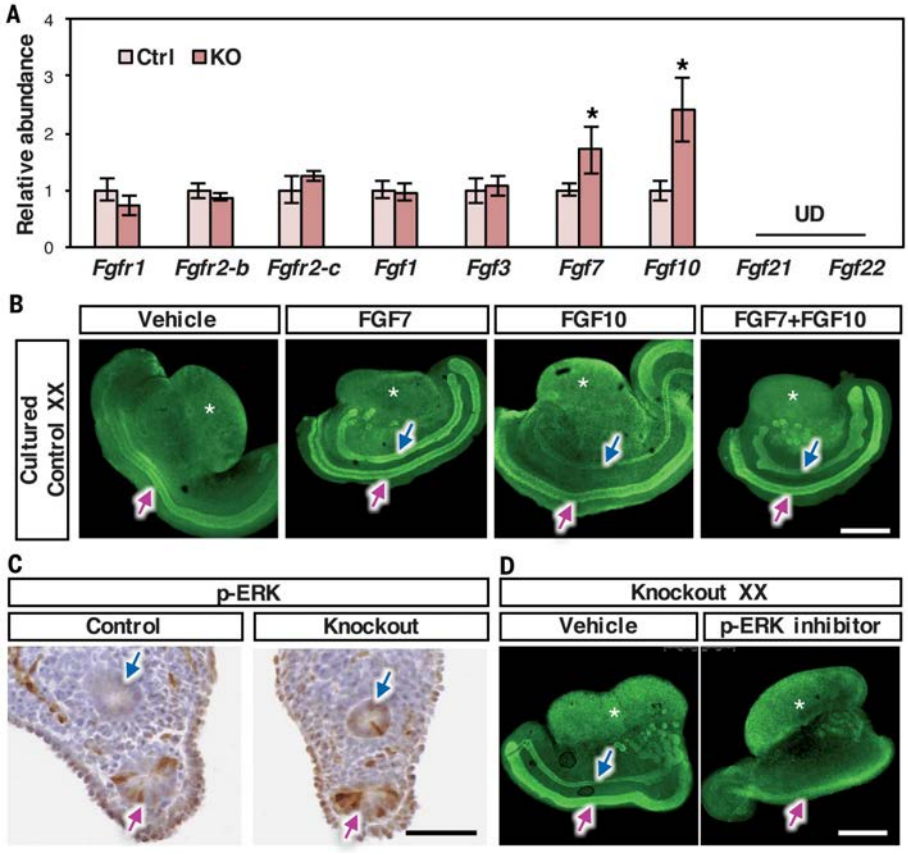

Fig. 3. Enhanced FGF signaling is involved in Wolffian duct retention in the absence of *Coup-tfII*. (**A**) mRNA expression of FGF receptors and ligands in the mesonephroi at E14.5. UD, undetected. Results are shown as mean ± SEM. Asterisks represent statistical significance of $P < 0.05$ compared with control females by using Student's *t* test ($n = 8$ embryos for each genotype). (**B**) Whole-mount immunofluorescence of PAX2 of 2-day cultured E14.5 wild-type XX mesonephroi in the presence of vehicle, or FGF7, FGF10, or FGF7+FGF10. (**C**) p-ERK immunohistochemistry of control and knockout XX mesonephroi at E14.5. (**D**) PAX2 whole-mount immunofluorescence in vehicle- or p-ERK inhibitor–treated knockout XX genital ridges. $n = 3$ embryos per group in (B) to (D). Scale bars, (B) and (D), 0.5 mm; (C) 50 μm. Blue arrows indicate Wolffian ducts, magenta arrows indicate Müllerian ducts, and white asterisk indicates ovary.

was not different between control and knockout XX mesonephroi (fig. S5A). Components of FGF signaling, in contrast, exhibited distinct changes in the absence of *Coup-tfII*. FGFR2 is the major FGF receptor in the Wolffian duct epithelium (*19*), and its binding ligands include FGF1, -3, -7, -10, -21, and -22 (*20*). mRNA expression of FGF receptors (*Fgfr1*, *Fgfr2-b*, and *Fgfr2-c*) and most ligands were unaltered (*Fgf1* and *Fgf3*) or undetectable (*Fgf21* and *Fgf22*) in knockout XX mesonephroi compared with the control (Fig. 3A). However, expression of *Fgf7* and *Fgf10* was increased significantly in knockout XX mesonephroi at E14.5 (Fig. 3A) and E16.5 (fig. S5B). To investigate whether FGF7 and FGF10 were capable of reproducing the Wolffian duct maintenance phenotype in the wild-type female, we cultured E14.5 wild-type XX mesonephroi for 2 days in the presence of vehicle, FGF7, FGF10, or FGF7+FGF10. In the vehicle-treated group, Wolffian ducts regressed after 2-day culture, similar to the in vivo situation. In contrast, presence of FGF7, FGF10, or FGF7+FGF10 maintained the Wolffian duct in the wild-type XX mesonephroi (Fig. 3B).

FGF7 and FGF10 are expressed in the mesonephric mesenchyme, the same cellular compartment as COUP-TFII (*21*, *22*). These FGFs bind FGFR2 in Wolffian duct epithelium and activate two intracellular signaling components, phosphorylated protein kinase B (p-AKT) and phosphorylated extracellular signal-regulated kinase (p-ERK) (*20*). Loss of *Coup-tfII* did not change p-AKT activation in Wolffian ducts (fig. S5C). The presence of p-ERK, conversely, became detected in Wolffian duct epithelium of knockout XX compared with the control XX at E14.5 (Fig. 3C) and E16.5 (fig. S5D). These results indicate that loss of mesenchymal *Coup-tfII* led to an enhanced activity of p-ERK signaling in Wolffian duct epithelium. We then tested whether elevated p-ERK signaling was the cause of Wolffian duct maintenance by culturing the *Coup-tfII* knockout mesonephroi with a p-ERK specific inhibitor PD0325901 (*23*). In the vehicle-treated group, Wolffian ducts in the knockout XX were maintained in culture. Conversely, the p-ERK inhibitor eliminated Wolffian ducts in the knockout XX mesonephroi (Fig. 3D), indicating that enhanced p-ERK signaling was involved in Wolffian duct retention in the *Coup-tfII* knockout XX embryo.

We have shown that instead of a passive process occurring as a result of the absence of androgens, elimination of the male reproductive tract in the female embryo is actively promoted by COUP-TFII through its action in the Wolffian duct mesenchyme. COUP-TFII in the mesenchyme inhibits expression of FGFs, which otherwise activate the p-ERK pathway in the Wolffian duct epithelium for its maintenance. The function of COUP-TFII in facilitating Wolffian duct elimination is not restricted to XX embryos; when the testis was removed from the *Coup-tfII* knockout XY mesonephros, Wolffian ducts remained present despite a lack of androgens (fig. S6). These findings reveal unexpected mechanisms underlying the dimorphic development of the Wolffian ducts via COUP-TFII. In addition, maintenance of male reproductive tracts without androgens prompts a reassessment of the role of androgens in this process, which presumably is to antagonize the action of COUP-TFII.

REFERENCES AND NOTES

1. A. Kobayashi, R. R. Behringer, *Nat. Rev. Genet.* **4**, 969–980 (2003).
2. A. Jost, *Arch. Anat. Microsc. Morphol. Exp.* **36**, 271–315 (1947).
3. A. Jost, *Recent Prog. Horm. Res.* **8**, 379–418 (1953).
4. M. Welsh, P. T. Saunders, N. I. Marchetti, R. M. Sharpe, *Endocrinology* **147**, 4820–4830 (2006).
5. M. B. Renfree, J. Fenelon, G. Wijayanti, J. D. Wilson, G. Shaw, *Dev. Biol.* **334**, 429–436 (2009).
6. G. R. Cunha *et al.*, *J. Androl.* **13**, 465–475 (1992).
7. A. Murashima *et al.*, *Endocrinology* **152**, 1640–1651 (2011).
8. S. J. Higgins, P. Young, G. R. Cunha, *Development* **106**, 235–250 (1989).
9. F. G. Petit *et al.*, *Proc. Natl. Acad. Sci. U.S.A.* **104**, 6293–6298 (2007).
10. J. F. Armstrong, K. Pritchard-Jones, W. A. Bickmore, N. D. Hastie, J. B. Bard, *Mech. Dev.* **40**, 85–97 (1993).
11. A. Jost, D. Price, R. G. Edwards, *Philos. Trans. R. Soc. Lond. B Biol. Sci.* **259**, 119–130 (1970).
12. C. Liu, J. Peng, M. M. Matzuk, H. H. Yao, *Nat. Commun.* **6**, 6934 (2015).
13. E. A. Mostaghel *et al.*, *Cancer Res.* **70**, 1286–1295 (2010).
14. E. M. Snyder, C. L. Small, Y. Li, M. D. Griswold, *Biol. Reprod.* **81**, 707–716 (2009).
15. M. H. Tan, J. Li, H. E. Xu, K. Melcher, E. L. Yong, *Acta Pharmacol. Sin.* **36**, 3–23 (2015).
16. M. Heikkilä *et al.*, *Endocrinology* **146**, 4016–4023 (2005).
17. A. Maeshima *et al.*, *J. Am. Soc. Nephrol.* **18**, 3147–3155 (2007).
18. C. Gupta, S. Siegel, D. Ellis, *Dev. Biol.* **146**, 106–116 (1991).
19. M. Okazawa *et al.*, *Dev. Biol.* **400**, 139–147 (2015).
20. N. Turner, R. Grose, *Nat. Rev. Cancer* **10**, 116–129 (2010).
21. P. W. Finch, G. R. Cunha, J. S. Rubin, J. Wong, D. Ron, *Dev. Dyn.* **203**, 223–240 (1995).
22. A. A. Thomson, G. R. Cunha, *Development* **126**, 3693–3701 (1999).
23. A. Akinleye, M. Furqan, N. Mukhi, P. Ravella, D. Liu, *J. Hematol. Oncol.* **6**, 27 (2013).

ACKNOWLEDGMENTS

We thank B. McIntyre, L. Roberts, and D. McClain for AGD measurement instruction, Wolffian duct culture instruction, and colony maintenance, respectively. This research was supported by the NIH Intramural Research Fund Z01-ES102965 to H.H.-C.Y., extramural research fund DK59820 and HL114539 to S.Y.T. and M.-J.T., and DK45641 to M.-J.T. Microarray data have been deposited in Gene Expression Omnibus under accession no. GSE100015.

SUPPLEMENTARY MATERIALS

www.sciencemag.org/content/357/6352/717/suppl/DC1
Materials and Methods
Figs. S1 to S6
Tables S1 and S2
References

30 August 2016; resubmitted 18 May 2017
Accepted 21 June 2017
10.1126/science.aai9136

Science

Elimination of the male reproductive tract in the female embryo is promoted by COUP-TFII in mice

Fei Zhao, Heather L. Franco, Karina F. Rodriguez, Paula R. Brown, Ming-Jer Tsai, Sophia Y. Tsai and Humphrey H.-C. Yao

Science **357** (6352), 717-720.
DOI: 10.1126/science.aai9136

The makings of the reproductive tract

Every embryo, regardless of its sex, contains both male and female primitive reproductive tracts before sexual differentiation. To establish a sex-specific reproductive system, female embryos need to remove the components of male tracts. The general consensus contends that removal of the male tracts occurs by default, a passive outcome owing to a lack of testis-derived androgens. Working in mice, Zhao *et al.* discovered that this process instead was actively promoted by the transcription factor COUP-TFII (see the Perspective by Swain). Without the action of this factor, embryos retained male reproductive tracts, independently of androgen action. These findings unveil unexpected mechanisms underlying the sexually dimorphic establishment of reproductive tracts.

Science, this issue p. 717; see also p. 648

Science (print ISSN 0036-8075; online ISSN 1095-9203) is published by the American Association for the Advancement of Science, 1200 New York Avenue NW, Washington, DC 20005. The title *Science* is a registered trademark of AAAS.

Original Article

Sexual Development

Sex Dev 2017;11:190–202
DOI: 10.1159/000477452

Accepted: March 28, 2017
by M. Schmid
Published online: July 27, 2017

Androgen Regulates Dimorphic F-Actin Assemblies in the Genital Organogenesis

Liqing Liu[a, b] Kentaro Suzuki[c] Eunice Chun[d] Aki Murashima[c, e] Yuki Sato[f] Naomi Nakagata[g] Toshihiko Fujimori[h] Shigenobu Yonemura[i] Wanzhong He[b] Gen Yamada[c]

[a]National Laboratory of Biomacromolecules, Institute of Biophysics, Chinese Academy of Sciences and [b]National Institute of Biological Sciences, Beijing, China; [c]Department of Developmental Genetics, Wakayama Medical University, Wakayama, Japan; [d]PIC Philippines, Inc., Pasig City, Philippines; [e]Division of Human Embryology, Department of Anatomy, Iwate Medical University, Nishitokuta Yahaba; [f]Department of Anatomy and Cell Biology, Kyushu University Graduate School of Medicine, Fukuoka, [g]Division of Reproductive Engineering, Center for Animal Resources and Development, Kumamoto University, Kumamoto, [h]Division of Embryology, National Institute for Basic Biology, Okazaki, and [i]Department of Cell Biology, Tokushima University Graduate School of Medical Science, Tokushima, Japan

Keywords
Cell migration · Extracellular matrix · F-actin · Masculinization programming window · Urethral mesenchymal cells

Abstract
Impaired androgen activity induces defective sexual differentiation of the male reproductive tract, including hypospadias, an abnormal formation of the penile urethra. Androgen signaling in the urethral mesenchyme cells (UMCs) plays essential roles in driving dimorphic urethral development. However, cellular events for sexual differentiation remain virtually unknown. In this study, histological analyses, fluorescent staining, and transmission electron microscopy (TEM) were performed to reveal the cellular dimorphisms of UMCs. F-actin dynamics and migratory behaviors of UMCs were further analyzed by time-lapse imaging. We observed a prominent accumulation of F-actin with poorly assembled extracellular matrix (ECM) in female UMCs. In contrast, thin fibrils of F-actin co-aligning with the ECM through membrane receptors were identified in male UMCs. Processes for dimorphic F-actin assemblies were temporally identified during an androgen-regulated masculinization programming window and spatially distributed in several embryonic reproductive tissues. Stage-dependent modulation of the F-actin sexual patterns by androgen in UMCs was also demonstrated by time-lapse analysis. Moreover, androgen regulates coordinated migration of UMCs. These results suggest that androgen signaling regulates the assembly of F-actin from cytoplasmic accumulation to membranous fibrils. Such alteration appears to promote the ECM assembly and the mobility of UMCs, contributing to male type genital organogenesis.

The reproductive organs possess the sexually specific structures to perform the reproductive function. External genitalia are one of the representative organs showing the sexual differences, with the penile urethra being responsible for copulation and urination in the male. The genital tubercle (GT) is the common anlage for the external genitalia of both the male and the female. Androgen regulates masculinization processes of the male reproductive organs contributing to the dimorphic development of the GT. 5α-dihydrotestosterone (DHT) is the

KARGER

E-Mail karger@karger.com
www.karger.com/sxd

Kentaro Suzuki or Gen Yamada
Department of Developmental Genetics, Wakayama Medical University
Kimiidera 811-1,Wakayama City
Wakayama 641-8509 (Japan)
E-Mail k-suzuki@wakayama-med.ac.jp or gensan7@wakayama-med.ac.jp

major androgen for GT masculinization. Testosterone (T) is converted into DHT in the ventral GT mesenchyme by the local 5α-reductase [Suzuki et al., 2017]. Mesenchymally-derived androgen signaling is indispensable for the formation of the penile urethra [Miyagawa et al., 2009]. Genetic and molecular mechanisms involved in androgen driven formation of the penile urethra have been studied [Yong et al., 2007; Miyagawa et al., 2009; Chen et al., 2010]. However, the mode of androgen actions regulating cellular differentiation of urethral mesenchymal cells (UMCs) in ventral GT remains to be elucidated.

Androgen actions are required in a specific time window, namely the masculinization programming window (MPW), to regulate multiple processes for the formation of male-type reproductive organs [Welsh et al., 2008, 2014]. Impaired activities of androgen actions within the MPW induce defective male sexual differentiation, such as hypospadias, prostate hypoplasia, and a shorter anogenital distance [Welsh et al., 2008; Suzuki et al., 2015]. Hypospadias is an ectopic opening of the penile urethra in the ventral external genitalia. The incidence of hypospadias ranges from 1:200~1:300 in male newborns [Manson and Carr, 2003; Cunha et al., 2015] and has been reported as increasing over the past few decades due to environmental exposure of anti-androgenic endocrine disruptors [Wilhelm and Koopman, 2006; Cunha et al., 2015]. The critical time window for urethral masculinization is from embryonic day 15.5 (E15.5) to E16.5 in mice [Miyagawa et al., 2009]. Improper exposure of androgen within the time window causes the several degrees of hypospadias. It remains largely unknown how androgen play roles in the differentiation of UMCs within the MPW.

Cytoskeletons regulate cell morphology and cell movement [Alberts, 2008; Heisenberg and Bellaiche, 2013]. The dynamics of actin assembly provide a mechanical basis for cellular behaviors, such as cell mobility and assembly of the extracellular matrix (ECM) [Blanchoin et al., 2014]. Cultured fibroblast cells have been one of the popular models to study cell biology in vitro [Grinnell, 2008; Friedl and Wolf, 2010; Luo et al., 2013]. However, how the assembling pattern of F-actin contributes to the function of mesenchymal fibroblasts during developmental processes remains poorly understood.

In the current study, we observed dynamic sexually different patterns of F-actin in UMCs during urethral formation. Such sexual patterns were regulated by androgen within the MPW. Furthermore, formation of dimorphic F-actin patterns was spatial-temporally consistent with the embryonic sexual differentiation processes of several reproductive organs. Of note, dimorphic assemblies of F-actin may correlate with the sexual differences of both ECM assemblies and migratory behaviors of UMCs. These results suggest that sexually different assemblies of F-actin may contribute to dimorphic reproductive organogenesis.

Materials and Methods

Animals

Mice expressing Actin-Venus (CDB0253K) and Lyn-Venus [Abe et al., 2011] under the control of the Rosa26 Loci were used for time-lapse imaging analysis of tissue slices. $AR^{Flox/Flox}$ [Sato et al., 2004] females were mated with CAG-Cre [Araki et al., 1997] males to obtain *AR* knockout males (AR^{Flox}/y: CAG^{Cre}, hereafter designated as ARKO males) [Murashima et al., 2011].

Histology

Hematoxylin and Eosin (H & E) and Masson Trichrome staining were performed by standard procedures as previously described [Ogi et al., 2005; Haraguchi et al., 2007]. Tissue sections were prepared into 6 μm in thickness for H & E staining and 4 μm for Masson's Trichrome staining.

F-Actin and Immuno-Fluorescent Staining for Confocal Microscopy

GT and other embryonic tissues at various stages were fixed in 1% PFA at 4°C for 1 h and rinsed and embedded in Cryomold (Tissue-TEK, Sakura, 4566) with OCT compound (Tissue-TEK, Sakura, 4583). Samples were frozen and stored at –80°C. Cryosections were dissected into 12 μm thickness by a freezing microtome (Leica CM1900), mounted on poly-lysin coated slides, dried briefly for 0.5 h at room temperature (RT), and were re-fixed with 1% PFA on ice for 20 min before staining. F-actin was stained with Alexa-488/647 phalloidin (Invitrogen) following the manufacturer's protocol. In the experiments of F-actin co-staining with other antibodies, phalloidin staining was performed during the secondary antibody incubation. Samples were dissected and fixed with 4% PFA at 37°C for α-tubulin staining. Antibodies for α-tubulin (Abcam, Ab52866; 1:300), vimentin (Sigma, V6630; 1:500), fibronectin (Sigma, F1141; 1:500), integrin α5 (BD Pharmingen, 553318; 1:500), and non-muscle myosin IIB (Biolegend, prb-445p; 1:500) were employed.

Chemically Fixed Sample Preparation and Transmission Electron Microscopy

Samples were fixed with 2.5% glutaraldehyde, 2% formaldehyde in 0.1 M sodium cacodylate buffer (pH 7.4) for 2 h at RT followed by post-fixation with ice-cold 1% OsO_4 in the same buffer for 2 h. After being stained en bloc with 0.5% uranyl acetate for 2 h or overnight at RT, samples were dehydrated with ethanol and propylene oxide and embedded in Poly/Bed 812 (Polyscience). Ultra-thin (70 nm) sections were double-stained with uranyl acetate and Reynold's lead citrate and examined under a JEOL JEM 1010 electron microscope at an accelerating voltage of 100 kV.

High-Pressure Freezing, Freeze-Substitution, and Transmission Electron Microscopy

Main procedures of sample preparation and transmission electron microscopy (TEM) analysis followed previous descriptions [He et al., 2003] with minor modification to adapt with a different target tissue. The pregnant host animals were anesthetized by isoflorane, and urethral tissues at the proximal GT with thickness <100 μm were dissected quickly from live embryos and mounted flatly on the 100 μm depth specimen carriers for high-pressure freezing. Excess space of the carrier chamber was filled with 20% lipid-rich BSA (ALBUMAXI, Gibco) to remove air bubbles. Specimen were frozen within 310~380 ms under ~2,050 bar high-pressure with HPF-compact-01 (Wohlwend GmbH) to obtain a vitrified fixation. The time from embryo dissection to freezing was limited within 40 s to maintain better physiological conditions. Samples were transferred into screw-typed tubes containing 1% OsO_4 and 0.1% uranyl acetate in acetone in liquid nitrogen and were subsequently transferred into a Leica EM AFS2 for freeze-substitution. Substitution was programmed as –90°C for 24 h, –60°C for 10 h, and –30°C for 18 h. Temperatures increased slowly during each transition for more than 2 h. Samples were washed 3 times with pure acetone after warming up slowly to 4°C and were subsequently warmed up to RT. Urethral tissues were carefully separated from the carrier and infiltrated with Epoxy resin (SPI PON, DDSA, and NMA from SPI-CHEM). Polymerization of resin was achieved by warming at 45°C for 18–24 h and 60°C for 48 h. Sections of 70 nm were placed on 200 mesh fine bar hexagonal grids (Ted Pella, Inc.) coated with a formvar membrane. Positive staining was performed by 3% uranyl acetate in 70% methanol on ice for 7 min and SATO lead in RT for 2 min. Images were recorded with Tecnai G2 Spirit (FEI Corp., Eindhoven, The Netherlands) equipped with 4 k × 4 k CCD camera (Gatan Corp.).

Urethral Tissue Slice Culture and Time-Lapse Imaging

GTs with its proximal perineum tissue were dissected at E14.5, E15.5, and E16.5, rinsed, and embedded in 4% low melting agarose gel (Funakoshi, LM-01) with the distal tip of the GT vertically upward. Agarose gel-fixed tissues were sectioned into slices of 150 μm thickness with a Vibratome 7000 (Campden Instrument, Smz). Sections of urethral tissues in the proximal GT were analyzed. Paired urethral tissues were used for comparisons of different treatments. Rat-tail collagen I (BD3542236) was diluted to 2% and modulated at ~pH 7.3 with osmotic pressure by 10× PBS (Wako), charcoal-stripped FBS (Hyclone), 0.05 M NaOH. Urethral tissue slices were rinsed with 2% collagen gel and mounted on a 4-well glass bottom dish (Matsunami, D141400). The membrane of the cell culture inserts (MilliCell, PIHT30R48) was prepared into pieces of 9 mm diameter and rinsed with collagen gel. Urethral tissue slices were covered with the culture insert membrane for a flat mounting to the glass bottom. Collagen gel was fixed at 37°C for 10 min. Additional 100 μl of 2% collagen gel was added to the membrane and fixed at 37°C for 1 h. A volume of 200 μl F12 (Gibco) containing 20% charcoal-stripped FBS was added to each culture well. A physiological concentration of DHT (10^{-8} M) was used for the culture. Chemical inhibitors employed in the slice culture system were latrunculin A (Invitrogen) at 5 μM and jasplakinolide (Invitrogen) at 5 μM.

Spinning disk microscopies (Cell Voyager CV-1000, Yokogawa) with 60× oil lenses were employed for time-lapse imaging experiments. The 10 μm sample depth, ranging from 5 to 15 μm from the bottom of the tissue slice, was imaged to trace the actin dynamics and cell movement.

Imaging Analysis

Imaris (Bitplane) was utilized to modulate the brightness and contrast as well as make 10 μm 3D projections and snapshots at various time points for the time-lapse imaging analysis of Actin-venus indicator mice.

Imaris was also utilized to detect, track, and visualize cell displacement for the time-lapse imaging analysis of Lyn-Venus membrane indicator mice. Cells within 100 × 100 μm scope in the center of each image were tracked, and tracks were manually validated and corrected. Imaris was also applied to obtain quantitative data for the parameter of Track_Speed_Mean, Track_Displacement_Length, and Track_Length. Such parameters were analyzed in Microsoft Excel to represent the velocity and straightness of the cell movement. Graphpad prism5 was utilized to assemble the cell migratory data.

Results

Sexually Dimorphic F-Actin Pattern in Genital Development

Gross morphological sexual difference of the GT becomes initially evident in its ventral side at E16.5 [Suzuki et al., 2002; Yamada et al., 2003a]. The formation of the penile urethra extended into the male GT, whereas it was not formed in the female GT (Fig. 1A, B). Androgen signaling in the mesenchyme around the urethra (hereafter designated as UMCs) is essential for the formation of the penile urethra [Miyagawa et al., 2009; Suzuki et al., 2014]. Intriguingly, cellular morphology of UMCs was significantly different between sexes (Fig. 1C–F). Male UMCs mostly displayed elongated spindle-like cell shape (Fig. 1D, white arrows in Fig. 1F). In contrast, female UMCs showed more rounded morphology (Fig. 1C, white arrows in Fig. 1E).

Cytoskeletons support the dynamic changes of cellular morphology. We thus analyzed the cytoskeletal components of the UMCs. F-actin staining indicates the structural dynamics of actin filaments. Thin F-actin fibrils were observed in male UMCs (Fig. 1I, I', J; online suppl. Video1b; see www.karger.com/doi/10.1159/000477452 for all online suppl. material). On the other hand, a prominently differential pattern of F-actin was observed in female UMCs. F-actin was accumulated into an intensely stained prominent granulation reaching to 2–6 μm in diameter. Such accumulation projected thick fibrils out from the central granule (Fig. 1G, G', H; online suppl. Video1a). Moreover, one UMC appeared to possess one such F-actin accumulation based on its number relative to the nuclei number of the UMCs (No. of accumula-

tions/no. of nuclei = 0.98 ± 0.09; 420 nuclei were counted, n = 6) (data not shown). Vimentin is one of the major components of intermediate filaments in mesenchymal cells, and α-tubulin is one of components of the subunit of the microtubule. Contrary to the prominent sexual differences of F-actin, neither the intermediate filaments nor the microtubule showed obvious sexual differences in UMCs (online suppl. Fig. 1A–H). These results suggest that the sexually dimorphic patterns of F-actin are associated with the dimorphic cellular shapes of UMCs. Next, we investigated sequentially the formation of F-actin assembly from E12.5 to postnatal day 35 (P35). Networks of F-actin fibrils were similarly observed in UMCs of both sexes earlier than E14.0 (Fig. 1K, L; data not shown). Sub-

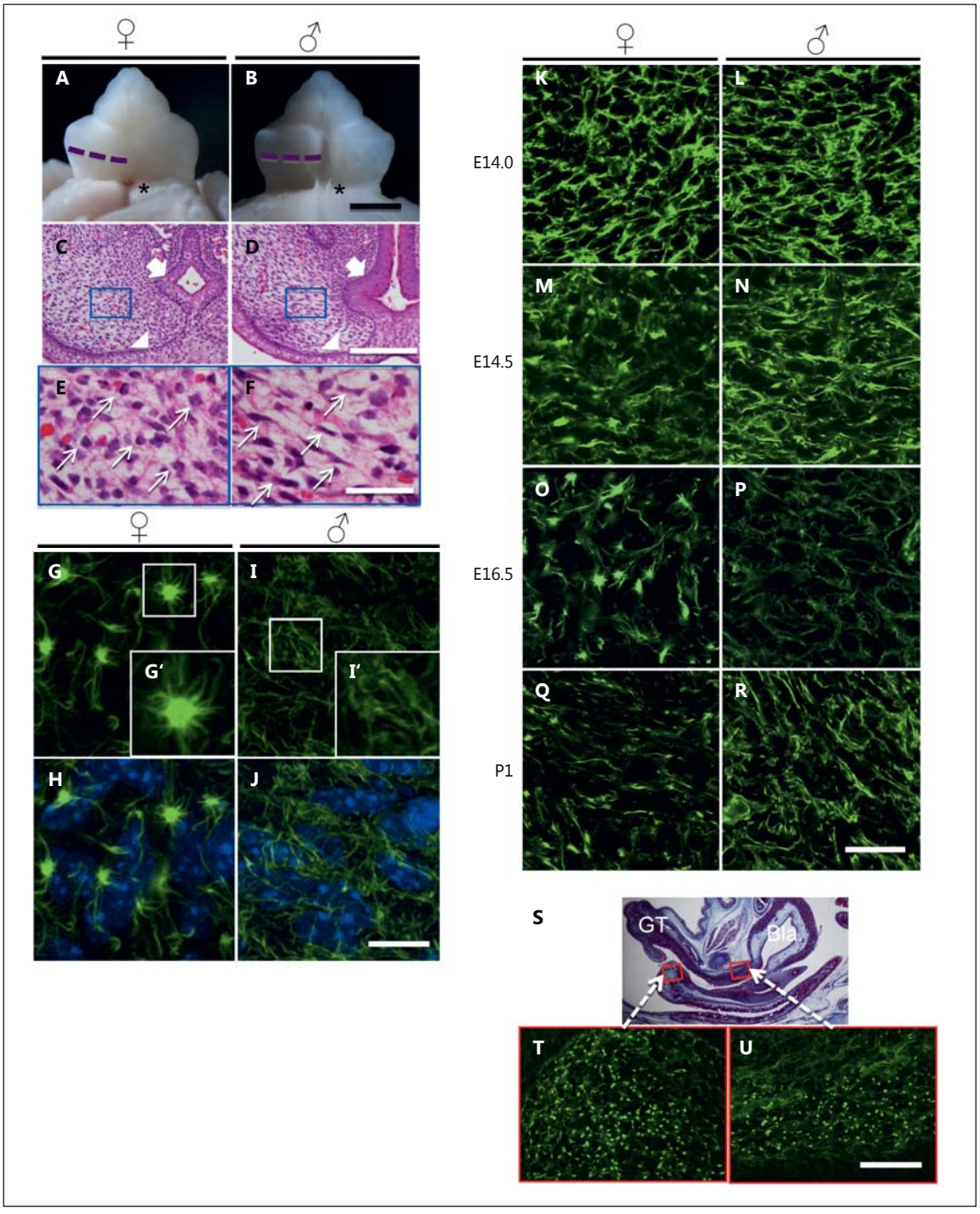

1

(For legend see next page.)

sequently, F-actin was assembled into accumulated structures in female UMCs (Fig. 1M) in contrast to the thinner fibrils in male UMCs (Fig. 1N) at E14.5. The most prominent sexual difference of the F-actin assembly was observed between E16.5 and E17.5. Obvious F-actin accumulations were formed in the female UMCs (Fig. 1O). In contrast, much thinner F-actin fibrils developed in the male UMCs (Fig. 1P). Such sexually dimorphic patterns were less prominent at postnatal day 1 (P1) (Fig. 1Q, R). Thereafter, sexual differences of the F-actin pattern become gradually diminished during the postnatal stages (data not shown).

In order to gain insight into the sexual differences of F-actin patterns, we analyzed the F-actin assembly in other tissues of the body trunk and limbs at E16.5. Similar sexual differences could be hardly observed in the skin and the limb mesenchyme (data not shown). However, F-actin accumulations were prominently detected in 2 mesenchymal regions of the female reproductive tract. One location is the lower part of the urethral mesenchyme adjacent to the orifice (Fig. 1S, T), and the other positive region was the upper part of urogenital sinus (UGS) mesenchyme adjacent to the bladder neck region (Fig. 1S, U). This region corresponds to the prostatic budding site in the male urogenital sinus [Hayward et al., 1996] as also suggested by the presence of epithelial budding structures in the corresponding male region at E17.5 (data not shown). On the other hand, no such F-actin accumulation was detected in the urogenital tract of the male. Male mesenchymal cells presented filamentous pattern of F-actin in the corresponding regions (data not shown). Thus, formation of F-actin accumulation appears to be a female-specific feature in several reproductive tissues. We designate herein such accumulation as female-type F-actin accumulation (FTFA).

Androgen Signaling Modulates Progressive F-Actin Sexual Differentiation in UMCs

Androgen signaling regulates the masculinization of the reproductive tract [Yamada et al., 2003a; Wilhelm and Koopman, 2006; Welsh et al., 2008]. In order to verify the effect of androgen on F-actin assembly, time-lapse imaging systems were developed by using urethral tissue slice cultures. The actin fluorescent indicator mouse line, Actin-Venus [Abe et al., 2011], was employed to trace the actin dynamics of the UMCs at E14.5. Female UMCs developed FTFA-like structures within 12 h without DHT (Fig. 2B). They gradually achieved a large population of FTFA until 48 h (Fig. 2C–E), whose pattern was similar with the condition at E16.5 (Fig. 1O). The male UMCs developed FTFA without DHT within 36 h of culture (Fig. 2K–O). In contrast, male UMCs gradually formed thin F-actin fibrils in 2 days culture with DHT (Fig. 2P–T). Similar thin F-actin fibrils were also formed in the female UMCs under the treatment of DHT (Fig. 2F–J). Without DHT, F-actin developed into the FTFA regardless of the sex origins of the urethral tissue slices. These results suggest that DHT modulated F-actin patterning into thin fibrils.

To further confirm the involvement of androgen signaling for the formation of the F-actin pattern, we analyzed the GT of androgen receptor (AR) knockout (KO) mice. AR KO males also showed a similar F-actin phenotype like the WT female (online suppl. Fig. 2I, M). Furthermore, administration of DHT could not lead to the formation of the thin F-actin fibrils from FTFAs in AR KO male (online suppl. Fig. 2N, O, P). These results suggest that androgen signaling is essential for the modulation of the F-actin pattern.

DHT modulates the F-actin pattern from the accumulated into the fibrillar form in the female UMCs at E14.5

Fig. 1. F-actin sexual differentiation in genital mesenchymal cells. **A**, **B** Gross morphology of the genital tubercle (GT) in female (**A**) and male (**B**) mice at E16.5. Asterisks mark the orifice of the urethra in the female (**A**) and the fused urethra in the male in the proximal GT (**B**). Scale bar, 500 μm. **C–F** H & E staining of the urethral tissues at the proximal level of the GT indicated by dashed lines in **A** and **B**. **E**, **F** Urethral mesenchymal cells (UMCs) framed in **C** and **D**. Arrows show the urethral epithelium and arrowheads the ectodermal epithelium (**C**, **D**). Female UMCs mostly display rounded cell bodies (**C**, **E**, arrows) and male ones display elongated cell bodies (**D**, **F**, arrows). Scale bars, 150 μm (**C**, **D**) and 50 μm (**E**, **F**). **G**, **G′**, **I**, **I′** Maximum projection of 6 μm thickness confocal images of F-actin stained by phalloidin-Alexa488 in the UMCs. **G′**, **I′** Enlarged views of the framed area in **G** and **I**. **H**, **J** Merged images of F-actin with nuclei. Prominent F-actin accumulation with multiple fibrils projected out from the center in the female UMCs (**G**, **G′**, **H**). Thin F-actin fibrils are formed in the male UMCs (**I**, **I′**, **J**). Scale bar, 10 μm. **K–R** Time-course of F-actin sexual differentiation in the UMCs. F-actin patterns in UMCs show no obvious sexual differences between E14.0 female (**K**) and male (**L**). There is a partially accumulated pattern in female (**M**), and bundled fibrillar pattern in male (**N**) at E14.5, prominent F-actin accumulations in female (**O**) and thin fibrils in male (**P**) at E16.5, and a less accumulated pattern in female (**Q**) and less thin fibrils in male (**R**) at P1 compared to E16.5 female and male. Scale bar, 10 μm. **S–U** Spatial presence of F-actin accumulation. **S** Masson staining of the female urogenital system. Accumulated F-actin staining is present in the lower portion of the urethral mesenchyme under the perineum region (**T**) and in the upper portion of the urogenital-sinus mesenchyme in the bladder (Bla) neck region (**U**). Scale bar, 50 μm.

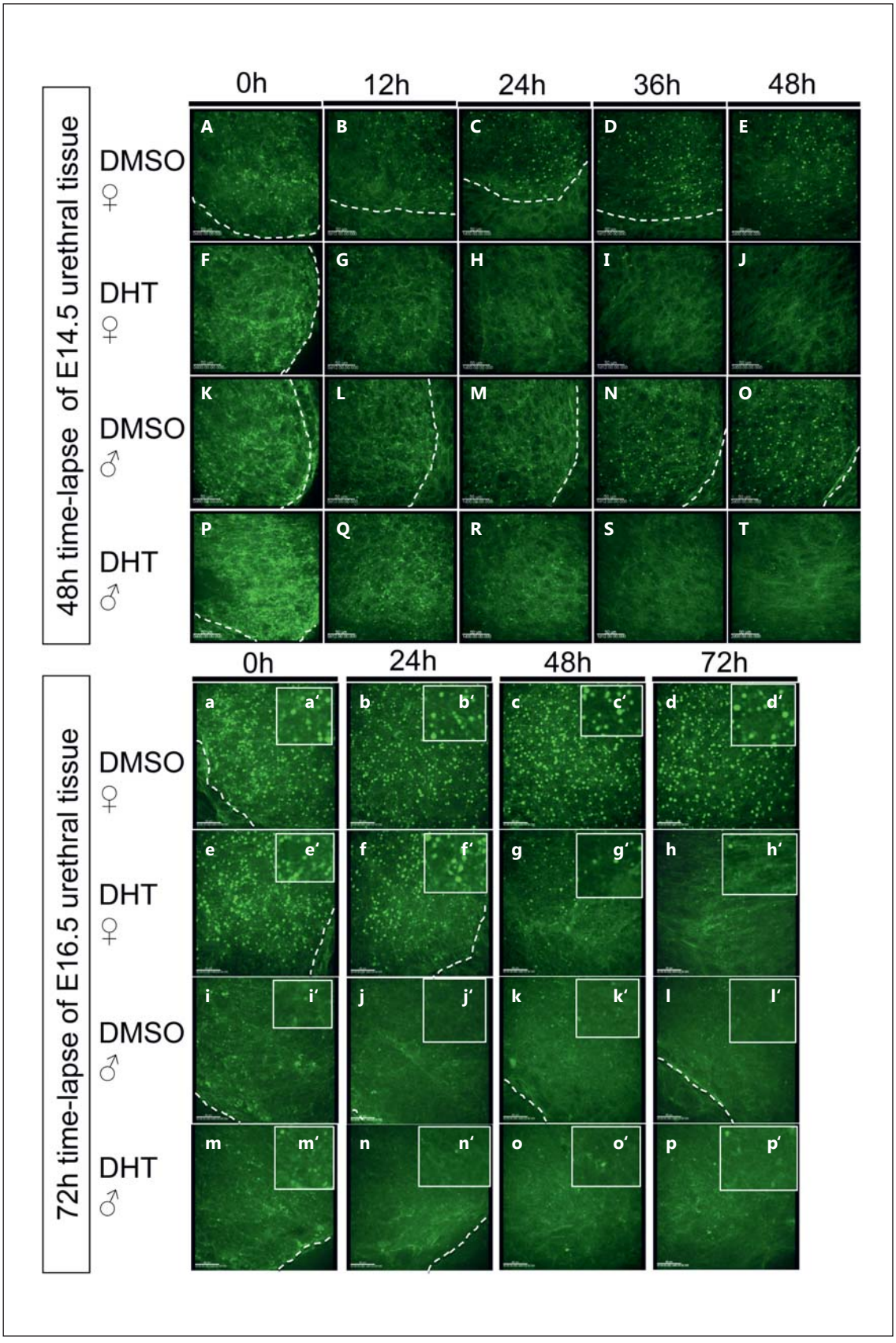

2

(For legend see next page.)

within 24 h (Fig. 2G, H). One day later, namely at E15.5, a longer time was necessary for such DHT-induced modulation of the F-actin pattern in female UMCs (online suppl. Fig. 2F, G, H). These results suggest that the duration of androgen exposure for modulating the F-actin pattern may depend on the developmental stage. To confirm the possibility, we evaluated the timespan to reverse the F-actin sexual pattern of E16.5 specimens. Some FTFAs still remained longer than 48 h of DHT treatment in female UMCs at E16.5 (Fig. 2g, g', h, h'). In the case of male UMCs, approximately 24 h were enough to form FTFA-like structures at E14.5 without DHT (Fig. 2M). However, almost no F-actin accumulations were formed even after 72 h culture of UMCs at E16.5 without DHT (Fig. 2l, l').

Dimorphic Assemblies of the Extracellular Matrix in UMCs

In order to get insights on the sexually dimorphic pattern of F-actin, we analyzed the subcellular localization of the F-actin structures by TEM. F-actin-like electron-dense structures were observed as the mass structure in the cytoplasm of female UMCs (Fig. 3A, area circled by white dashed line in Fig. 3C). Bundle-like structures were observed adjacent to the plasma membrane of the male UMCs (Fig. 3B, arrowheads in Fig. 3D). The physiological status of the cell can be preserved by fast cryo-fixation with high-pressure freezing followed by dehydration through freeze-substitution to reduce extraction of cellular contents [He et al., 2003; McDonald, 2014]. To further characterize dimorphic F-actin assembly, such samples were analyzed by TEM. Electron-dense mass structure was similarly observed in female UMCs (area circled by white dashed lines in Fig. 3E, G). Such FTFA-like structures occupied a large portion of cytoplasmic space, almost devoid of other subcellular organelles inside the FTFA (Fig. 3E, G). Visible F-actin bundles in male UMCs were likely formed adjacent to the plasma membrane (Fig. 3F, H, arrowheads). Such membranous localization of F-actin in the male may promote the physical interaction of the UMC with the ECM in the male.

Fibronectin, one of the key ECM components of mesenchymal fibroblasts, transduces mechanical forces between the intracellular cytoskeleton and the ECM through its membrane receptor, integrin α5β1 [Pankov and Yamada, 2002]. Fibronectin was assembled into fibrils, which co-aligned with the F-actin fibrils in the male UMCs (Fig. 4C, D, I, J, L; arrows), whereas fibronectin represented a patchy and non-linearized form in female UMCs (Fig. 4A, B, E, F, H). Prominent staining of integrin α5 was detected between the co-aligned fibrils of intracellular F-actin and extracellular fibronectin in male UMCs (Fig. 4K, L; arrows). In contrast, integrin α5 staining was barely observed between scarcely existing F-actin- and fibronectin-fibrils in the female UMCs (Fig. 4G, H; arrows). These results suggest the presence of more associations of F-actin structures with ECM in the male UMCs.

DHT Regulates Coordinated and Efficient Migration of UMCs

Dimorphic assemblies of both F-actin and the ECM indicated that there may be sexually different cellular behaviors of UMCs. To investigate this possibility, we analyzed the cellular behaviors of UMCs. Some UMCs migrated from the GT tissue slice into the collagen gel after 48 h culture of E14.5 specimens. We traced the behaviors of such UMCs derived from Actin-Venus indicator mice. Female UMCs moved randomly and barely contacted each other (online suppl. Video 2a). In contrast, female

Fig. 2. Stage-dependent regulation of F-actin sexual differentiation by androgen through the time-lapse imaging analyses of Actin-Venus indicator mice. **A–T** Imaging snapshots of E14.5 urethral tissue slices of female (**A–J**) and male (**K–T**) cultured with (**F–J**, **P–T**) or without (**A–E**, **K–O**) 10^{-8} M dehydrotestosterone (DHT) in 48 h. Female UMCs at E14.5 develop some F-actin accumulations within 12 h (**B**) and gradually achieve a large population of F-actin accumulation within 48 h (**C–E**) without DHT (DMSO vehicle control). Female UMCs at E14.5 gradually develop thin F-actin fibrils with DHT (**F–J**). Male UMCs at E14.5 develop a few F-actin accumulations at 24 h (**M**) and achieve a large population of F-actin accumulations at 48 h without DHT (**O**). Male UMCs gradually develop thin F-actin fibrils with DHT (**P–T**). **a–d** Imaging snapshots of E16.5 female (**a–h**) and male (**i–p**) urethral tissue slices cultured with (**e–h**, **m–p**) or without (**a–d**, **i–l**) 10^{-8} M DHT in 72 h. **a′–p′** Enlarged views of the central areas of **a–p**. Prominent F-actin accumulations of E16.5 female UMCs at 0 h (**a**, **a′**) were maintained in 72 h culture without DHT (**b**, **b′–d**, **d′**). Prominent F-actin accumulations of E16.5 female UMCs at 24 h (**e**, **e′**) are gradually reformed into thin fibrils (**f**, **f′–h**, **h′**), and a few remnants of F-actin accumulation remain at 72 h (**h**, **h′**) in the culture with DHT. Thin F-actin fibrils in E16.5 male UMCs at 0 h (**i**, **i′**) were basically maintained in the 72 h culture without DHT (**j**, **j′–l**, **l′**). Thin F-actin fibrils of E16.5 male UMCs (**m**, **m′**) were maintained in the 72 h culture with DHT (**n**, **n′–p**, **p′**). All images are Z-stalk projections of 10 μm thickness (11 slices, step-height 1 μm). Dashed lines, epithelial mesenchymal border. Scale bars, 50 μm.

UMCs associated and tended to migrate as a group when treated with DHT (online suppl. Video 2b). Male UMCs showed coordinated movements similar with the female UMCs in a DHT-treated condition (online suppl. Video 2d). However, male UMCs without DHT treatment migrated randomly and discretely (online suppl. Video 2c). These results indicate that DHT may promote coordinated cell behaviors of UMCs.

To further investigate the sexual differences of the migratory behaviors of the UMCs, Lyn-Venus membrane indicator mice [Abe et al., 2011] were employed to trace the individual cell movement in urethral tissue slices (Fig. 5; online suppl. Video 3). Male UMCs mostly migrated to the direction of the urethral epithelium (indicated as red line in Fig. 5 A–D), especially with DHT (Fig. 5B, D). However, female UMCs mostly migrated in

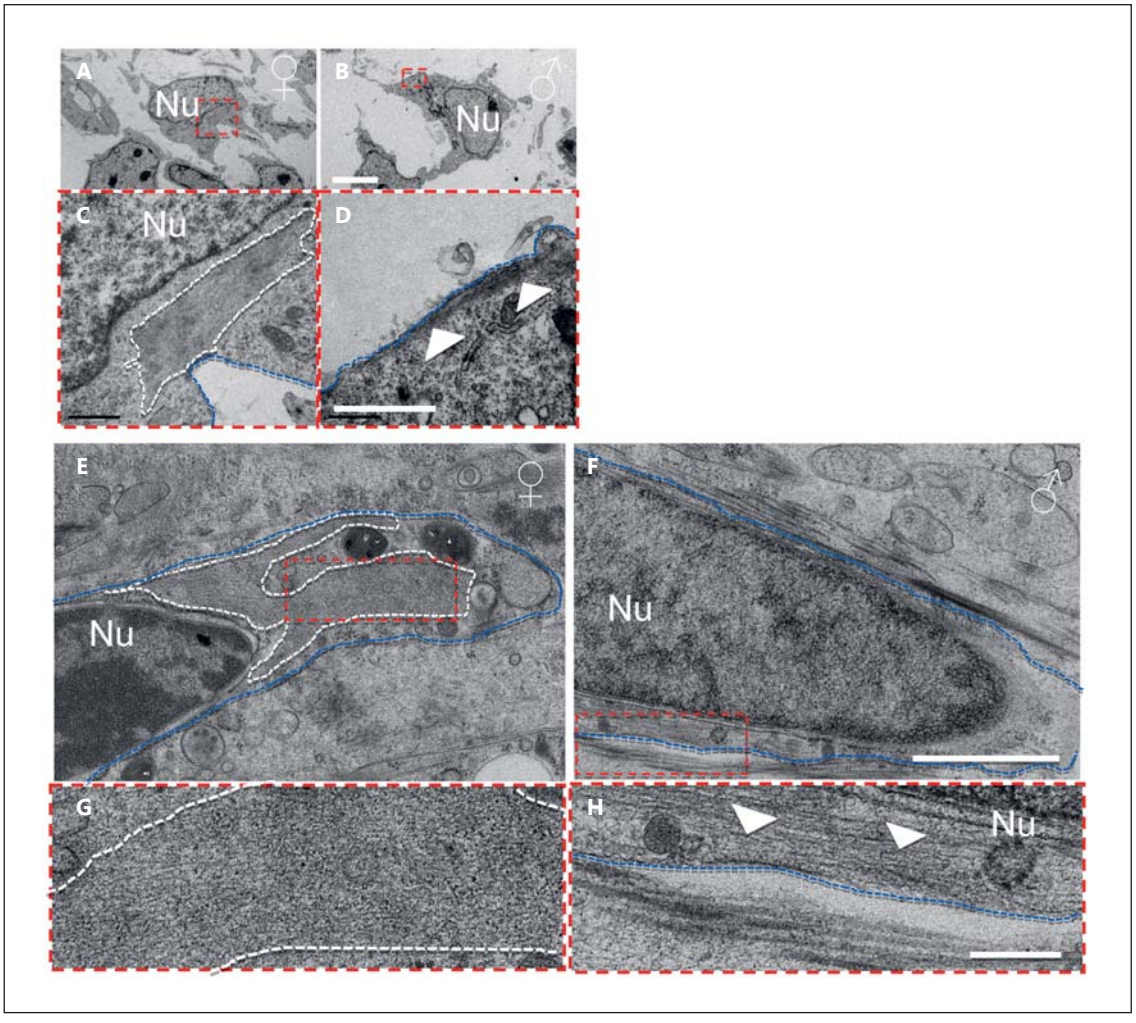

Fig. 3. Dimorphic assemblies of actin filament revealed by transmission electron microscopy (TEM). **A–D** Chemical-fixed electron microscopy showed the sex-differentiated status of F-actin. An electron-dense mass structure located in the cytoplasm was observed in the female UMCs (**C**, encircled by a white dashed line). The most prominent bundle-like actin structure was observed underneath the plasma membrane (**B**, **D**). The arrowheads point to F-actin structures in male UMCs (**D**), and blue dashed lines show the plasma membranes. Nu, Nucleus. Scale bars, 5 μm (**A**, **B**) and 1 μm (**C**, **D**). **E–H** High-pressure freezing, freeze substitution, and electron microscopy showed sex-differentiated status of F-actin in UMCs. The F-actin structure occupied a large portion of the cytoplasmic area (encircled by white dashed lines in **E** and enlarged in **G**), devoid of other cellular organelles inside the FTFA-like structure in the female UMC (**E**, **G**). F-actin bundles are located adjacent to the plasma-membrane in the male UMC (**F**, **H**). Arrowheads point to F-actin structures in male UMCs (**H**), and blue dashed lines show the plasma membranes. Nu, Nucleus. Scale bars, 1 μm (**E**, **F**) and 200 nm (**G**, **H**).

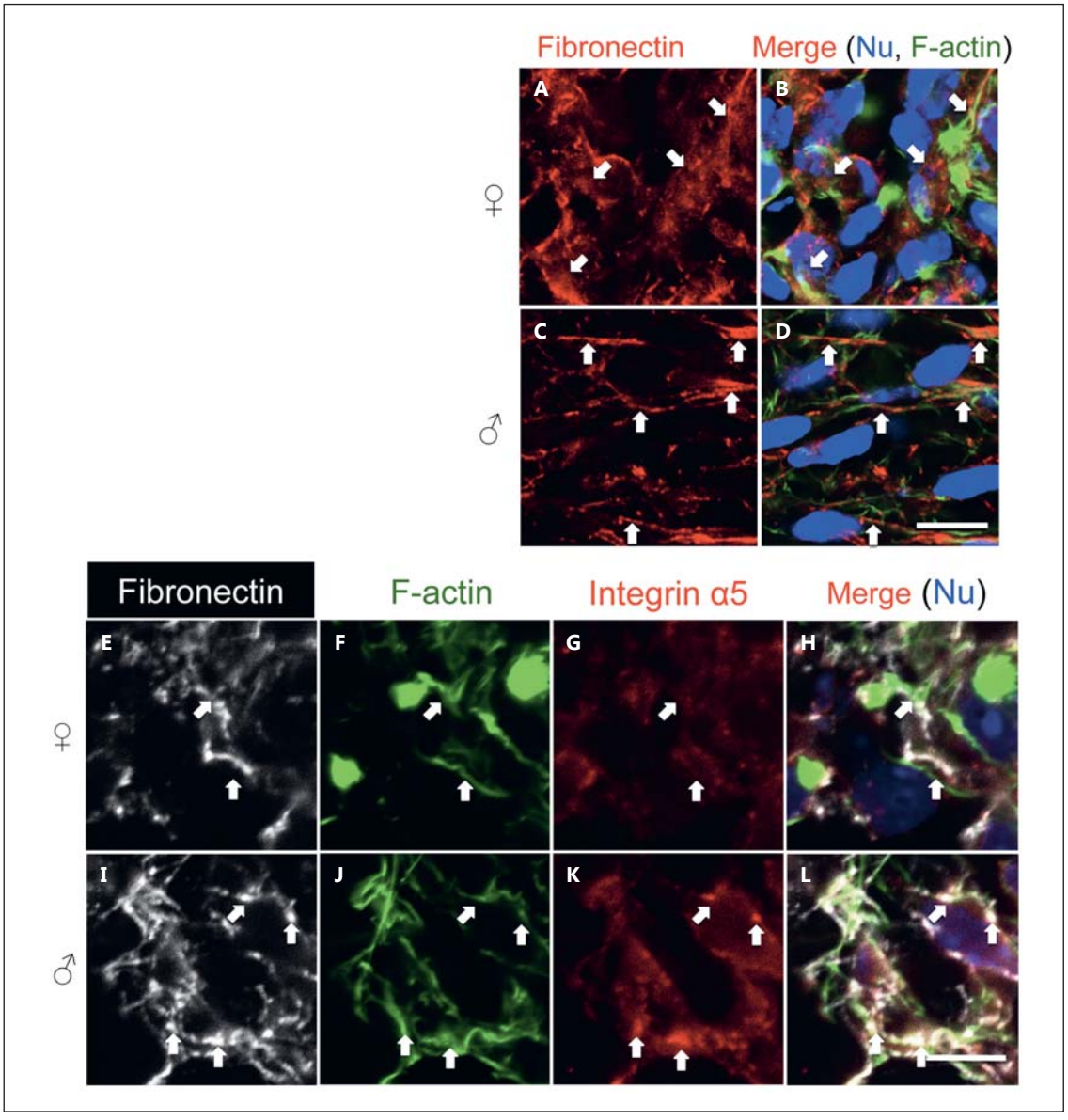

Fig. 4. More prominent co-alignment of fibronectin and F-actin in male UMCs. **A–D** Expression pattern of fibronectin of E16.5 UMCs. **B**, **D** Merged images of fibronectin (**A**, **C**) with F-actin (green) and nucleus (blue). Fibronectin presented a patchy and disorganized form (**A**), with few thick fibrils colocalized with FTFA in female UMCs (**B**). Fibronectin was assembled into fibrils (**C**), which co-aligned with the F-actin fibrils in male UMCs (**D**). Arrows show selective sites of fibronectin distribution. Scale bar, 10 μm. Immuno-fluorescent staining of fibronectin (**E**, **I**), F-actin (**F**, **J**), integrin α5 (**G**, **K**), and merged image of 3 fluorescence stainings with nucleus staining (**H**, **L**). Fibronectin of male UMCs (**I**) present a mostly fibrillar phenotype, co-aligned with intracellular F-actin (**J**, **L**), and there is prominent clustering of integrin α5 between the fibrils of F-actin and fibronectin as indicated by arrows (**K**, **L**). Fibronectin of female UMCs present a patchy form (**E**), barely colocalized with F-actin structures (**F**, **H**), and there is no prominent integrin α5 staining between the fibrils of fibronectin and F-actin as indicated by arrows (**G**, **H**). Scale bar, 5 μm.

random directions (Fig. 5A). The order of moving velocity of UMCs from low to high was female without DHT, female with DHT, male without DHT, and male with DHT (Fig. 5E). Straightness represents the ratio of displacement to the total migrating distance, which indicates the efficiency of the cell movement in one direction. The order of straightness was female without DHT, female with DHT, male without DHT, and male with DHT as the

Sex Dev 2017;11:190–202
DOI: 10.1159/000477452

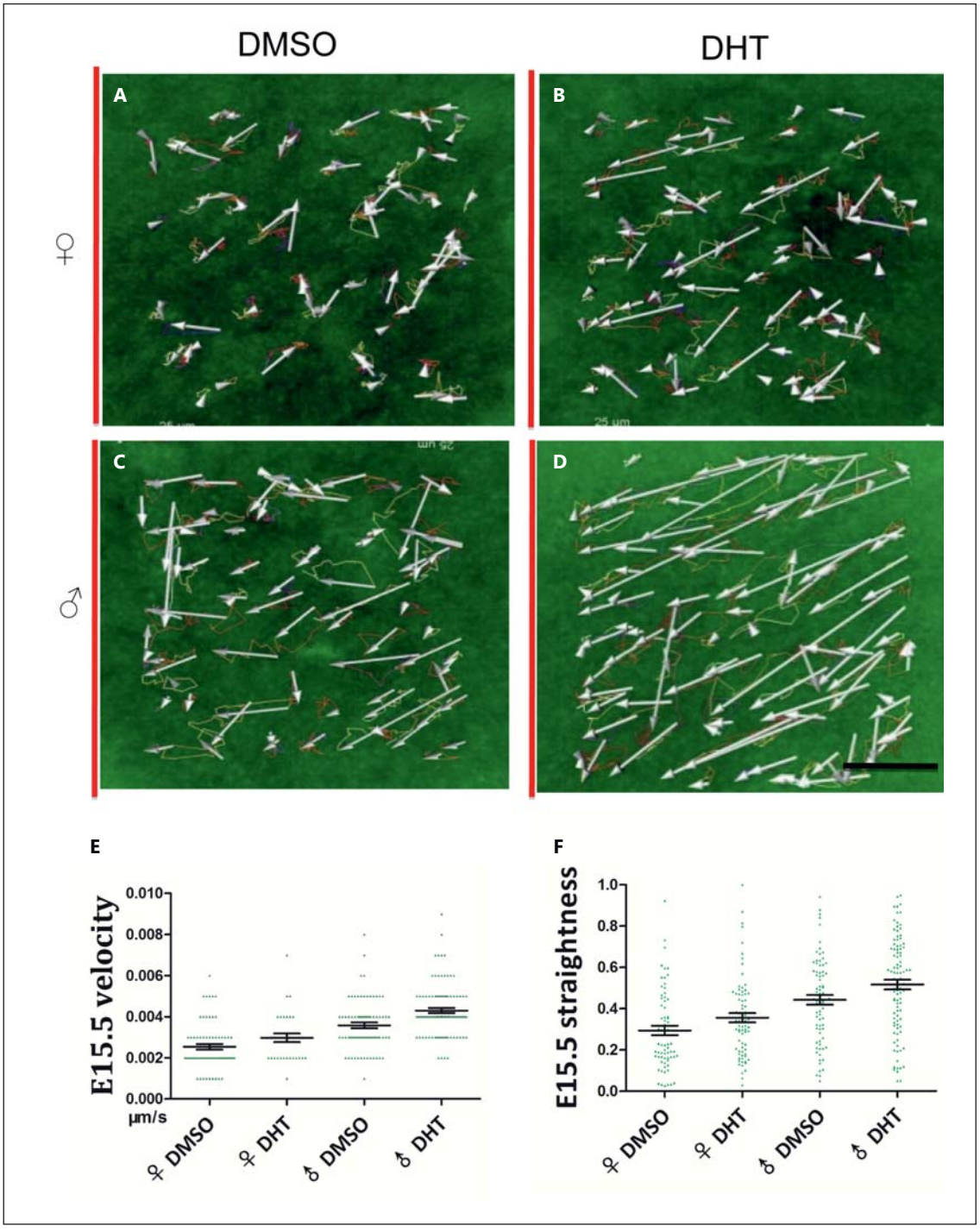

Fig. 5. Androgen regulates more rapid and directional movement of the UMCs. Movement of UMCs in 12-h time-lapse imaging of E15.5 urethral tissue slices from Lyn-Venus membrane indicator mice was traced by Imaris software. Moving route of the UMCs of female (**A**, **B**) or male (**C**, **D**) with (**B**, **D**) or without (**A**, **C**) DHT is displayed by both moving tracks (colored curved lines) and displacement (arrows). Scale bar, 25 μm. The urethral epithelium is arranged to the left side of urethral tissue slices and is indicated by red lines in **A–D**. Female UMCs without androgen treatment migrate randomly in all directions (**A**). Male UMCs with androgen treatment migrate coordinately to the urethral epithelium (**D**). **E** Velocity and **F** straightness (displacement/length of moving tracks) of UMCs movement are displayed with dispersing point graph. Average velocities of the cells are as follows: female DMSO = 0.0025 μm/s; female DHT = 0.0028 μm/s; male DMSO = 0.0036 μm/s; male DHT = 0.0043 μm/s. Average values of straightness for each group are as follows: female DMSO = 0.29; female DHT = 0.36; male DMSO = 0.44; male DHT = 0.52.

highest (Fig. 5F), which showed a similar tendency with the order of moving velocity. These results indicate that DHT may induce the more efficient and coordinated mobility of the UMCs to the urethral epithelium.

Discussion

Androgen Regulates the Sexually Dimorphic F-Actin Pattern

The current results indicate that the F-actin pattern in UMCs shows sexual differences and that androgen signaling is involved in the formation of such pattern. AR function in the mesenchyme is indispensable for fetal sexual differentiation of genital organs in the reproductive tract [Miyagawa et al., 2009]. AR was expressed in the UMCs more prominently in the male between E14.5 to E16.5 [Miyagawa et al., 2009; data not shown]. Secretion of testicular androgen from E13.0 initiates activities of androgen signaling in male embryos [O'Shaughnessy et al., 2006; Dean et al., 2012]. The sexually dimorphic F-actin assemblies in UMCs became initially distinguishable at E14.5, evident at E15.5 and E16.5. The critical time window for the dimorphic development of the GT in mice is reported from E15.5 to E16.5 [Miyagawa et al., 2009]. Sexually dimorphic F-actin patterns were formed around the timing of the MPW. A current study showed that the sexually dimorphic pattern of F-actin was reversible. However, the duration to accomplish sex-reversal patterns of F-actin appeared to depend on the developmental stage. Longer exposure time to modulate androgen signaling was necessary to reverse the female F-actin pattern in late stage (E16.5, more than 3 days) than in earlier stages (E14.5, within 1 days; E15.5, within 2 days). These results suggest that the mesenchymal response to androgen may be different in each stage. Of note, hypospadias-like phenotypes could be induced by anti-androgenic chemicals in the early and mid-stages of the MPW but not in the late MPW [Welsh et al., 2008]. Further analyses are required to understand the correlation between abnormal urethral formation and defects of the F-actin pattern formation.

Sexually dimorphic F-actin patterns were formed not only in the UMCs but also in the mesenchyme of some other embryonic genital regions, including the UGS adjacent to the bladder neck region and the anterior portion of the perineum. These 2 regions also show androgen-dependent masculinization such as prostate budding and perineum elongation. Furthermore, sexually dimorphic patterns of F-actin in the above reproductive tissues were formed at similar embryonic stages in the MPW. Taken together, the spatio-temporal programs of the formation of sexually dimorphic F-actin patterns may contribute to the sexual differentiation of several reproductive tissues.

Sexually Dimorphic F-Actin Patterns Possibly Regulate Distinct Behaviors of UMCs

The F-actin organizations provide a cellular basis for the contractive machineries of the cell to assemble the ECM [Ennomani et al., 2016]. The prominent presence of FTFA may attenuate the membranous distribution of F-actin networks, which may decrease the ability of the cell to associate with the ECM. Such a situation might lead to a poor assembly of the ECM in female UMCs.

Fibronectin binds to the cell membrane by its receptor, integrin α5β1, and regulates the assembly of several other ECM proteins [Pankov and Yamada, 2002; Yamada et al., 2003b]. The expression of integrin α5 between co-aligned F-actin and fibronectin fibrils indicated close associations of fibronectin and F-actin in male UMCs. Such association of F-actin fibrils with fibronectin may transduce mechanical properties from the cell to the ECM facilitating the assembly of the ECM adjacent to the plasma membrane of male UMCs [Yamada et al., 2003b; Alberts, 2008; Leiss et al., 2008]. Well-assembled ECM aligning along cell bodies might promote cellular behaviors of male UMCs in favor of their directional movement.

DHT promoted coordinated cell migration of UMCs in isolated collagen gel environments. Moreover, UMCs migrated more efficiently toward the urethral epithelium of the urethral tissue slices with DHT treatment. Such migration appeared to occur synergistically with a DHT-induced alteration of F-actin patterns. Furthermore, actin polymerization toxins, such as latrunculin A and jasplakinolide, diminished the F-actin sexual patterns and abolished the mobility of UMCs at the same time (data not shown). Thus, sexually dimorphic patterns of F-actin could play roles in the coordinated directional movement under androgen actions. The formation of the penile urethra involves a dynamic rearrangement of the urethral epithelium, such as the fusion of the urethral plate and the internalization of the urethral tube in the glans. Coordinated migration of UMCs toward the urethral epithelium might positively contribute to such active morphogenetic processes.

Advances in genetic and molecular studies promote the understanding of the mechanism of genital sexual differentiation. Several genes have been identified as essential regulators of male- and female-type reproductive organ formation [Miyagawa et al., 2009; Chen et al., 2010; Chen et al., 2011; Suzuki et al., 2014]. However, the cel-

lular level of differentiation, particularly mesenchymal characters in the male- and female-type genital organ formation processes remain unelucidated. Dimorphic F-actin assembly in genital organogenesis might be one of the cellular mechanisms for sexual differentiation of reproductive tissues. Further studies are required to reveal the molecular mechanisms of sexually different assemblies of F-actin regulated by androgen.

Acknowledgments

We thank Drs Benjamin Odermatt, Robert S. Adelstein, Toru Miyazaki, Takashi Seki, Jun Hatakeyama, Nan Tang for their invaluable support, and T. Iba for assistance. We also thank CDB laboratory for Animal Resources and Genetic Engineering for the source of the indicator mice. This work was supported by the Japan Society for the Promotion of Science KAKENHI Grant Numbers 15H04300, 15K15403 and 15K10647, also by China MOST (973 programs, 2011CB812502, 2014CB849902), and the Beijing Municipal Government.

Statement of Ethics

All experimental procedures and protocols were approved by the Committee on the Animal Research at the Kumamoto University (B22-198, A23-076), Wakayama Medical University (798), Japan, and by National Institute of Biological Science, Beijing, China (0013).

Disclosure Statement

The authors have no conflicts of interest to declare.

References

Abe T, Kiyonari H, Shioi G, Inoue K, Nakao K, et al: Establishment of conditional reporter mouse lines at rosa26 locus for live cell imaging. Genesis 49:579–590 (2011).

Alberts B: Molecular Biology of the Cell, ed 5 (Garland Science, New York 2008).

Araki K, Imaizumi T, Okuyama K, Oike Y, Yamamura K: Efficiency of recombination by cre transient expression in embryonic stem cells: comparison of various promoters. J Biochem 122:977–982 (1997).

Blanchoin L, Boujemaa-Paterski R, Sykes C, Plastino J: Actin dynamics, architecture, and mechanics in cell motility. Physiol Rev 94:235–263 (2014).

Chen H, Yong W, Hinds TD Jr, Yang Z, Zhou Y, et al: Fkbp52 regulates androgen receptor transactivation activity and male urethra morphogenesis. J Biol Chem 285:27776–27784 (2010).

Chen N, Harisis GN, Farmer P, Buraundi S, Sourial M, et al: Gone with the wnt: the canonical wnt signaling axis is present and androgen dependent in the rodent gubernaculum. J Pediatr Surg 46:2363–2369 (2011).

Cunha GR, Sinclair A, Risbridger G, Hutson J, Baskin LS: Current understanding of hypospadias: relevance of animal models. Nat Rev Urol 12:271–280 (2015).

Dean A, Smith LB, Macpherson S, Sharpe RM: The effect of dihydrotestosterone exposure during or prior to the masculinization programming window on reproductive development in male and female rats. Int J Androl 35:330–339 (2012).

Ennomani H, Letort G, Guerin C, Martiel JL, Cao W, et al: Architecture and connectivity govern actin network contractility. Curr Biol 26:616–626 (2016).

Friedl P, Wolf K: Plasticity of cell migration: a multiscale tuning model. J Cell Biol 188:11–19 (2010).

Grinnell F: Fibroblast mechanics in three-dimensional collagen matrices. J Bodyw Mov Ther 12:191–193 (2008).

Haraguchi R, Motoyama J, Sasaki H, Satoh Y, Miyagawa S, et al: Molecular analysis of coordinated bladder and urogenital organ formation by hedgehog signaling. Development 134:525–533 (2007).

Hayward SW, Baskin LS, Haughney PC, Foster BA, Cunha AR, et al: Stromal development in the ventral prostate, anterior prostate and seminal vesicle of the rat. Acta Anat 155:94–103 (1996).

He W, Cowin P, Stokes DL: Untangling desmosomal knots with electron tomography. Science 302:109–113 (2003).

Heisenberg CP, Bellaiche Y: Forces in tissue morphogenesis and patterning. Cell 153:948–962 (2013).

Leiss M, Beckmann K, Giros A, Costell M, Fassler R: The role of integrin binding sites in fibronectin matrix assembly in vivo. Curr Opin Cell Biol 20:502–507 (2008).

Luo W, Yu CH, Lieu ZZ, Allard J, Mogilner A, et al: Analysis of the local organization and dynamics of cellular actin networks. J Cell Biol 202:1057–1073 (2013).

Manson JM, Carr MC: Molecular epidemiology of hypospadias: review of genetic and environmental risk factors. Birth Defects Res A Clin Mol Teratol 67:825–836 (2003).

McDonald KL: Rapid embedding methods into epoxy and Lr White resins for morphological and immunological analysis of cryofixed biological specimens. Microsc Microanal 20:152–163 (2014).

Miyagawa S, Satoh Y, Haraguchi R, Suzuki K, Iguchi T, et al: Genetic interactions of the androgen and wnt/beta-catenin pathways for the masculinization of external genitalia. Mol Endocrinol 23:871–880 (2009).

Murashima A, Miyagawa S, Ogino Y, Nishida-Fukuda H, Araki K, et al: Essential roles of androgen signaling in Wolffian duct stabilization and epididymal cell differentiation. Endocrinology 152:1640–1651 (2011).

Ogi H, Suzuki K, Ogino Y, Kamimura M, Miyado M, et al: Ventral abdominal wall dysmorphogenesis of *msx1/msx2* double-mutant mice. Anat Rec A Discov Mol Cell Evol Biol 284:424–430 (2005).

O'Shaughnessy PJ, Baker PJ, Johnston H: The foetal Leydig cell– differentiation, function and regulation. Int J Androl 29:90–95; discussion 105–108 (2006).

Pankov R, Yamada KM: Fibronectin at a glance. J Cell Sci 115:3861–3863 (2002).

Sato T, Matsumoto T, Kawano H, Watanabe T, Uematsu Y, et al: Brain masculinization requires androgen receptor function. Proc Natl Acad Sci USA 101:1673–1678 (2004).

Suzuki H, Suzuki K, Yamada G: Systematic analyses of murine masculinization processes based on genital sex differentiation parameters. Dev Growth Differ 57:639–647 (2015).
Suzuki H, Matsushita S, Suzuki K, Yamada G: 5alpha-dihydrotestosterone negatively regulates cell proliferation of the periurethral ventral mesenchyme during urethral tube formation in the murine male genital tubercle. Andrology 5:146–152 (2017).
Suzuki K, Ogino Y, Murakami R, Satoh Y, Bachiller D, Yamada G: Embryonic development of mouse external genitalia: insights into a unique mode of organogenesis. Evol Dev 4: 133–141 (2002).
Suzuki K, Numata T, Suzuki H, Raga DD, Ipulan LA, et al: Sexually dimorphic expression of Mafb regulates masculinization of the embryonic urethral formation. Proc Natl Acad Sci USA 111:16407–16412 (2014).
Welsh M, Saunders PT, Fisken M, Scott HM, Hutchison GR, et al: Identification in rats of a programming window for reproductive tract masculinization, disruption of which leads to hypospadias and cryptorchidism. J Clin Invest 118:1479–1490 (2008).
Welsh M, Suzuki H, Yamada G: The masculinization programming window. Endocr Dev 27: 17–27 (2014).
Wilhelm D, Koopman P: The makings of maleness: towards an integrated view of male sexual development. Nat Rev Genet 7:620–631 (2006).
Yamada G, Satoh Y, Baskin LS, Cunha GR: Cellular and molecular mechanisms of development of the external genitalia. Differentiation 71:445–460 (2003a).
Yamada KM, Pankov R, Cukierman E: Dimensions and dynamics in integrin function. Braz J Med Biol Res 36:959–966 (2003b).
Yong W, Yang Z, Periyasamy S, Chen H, Yucel S, et al: Essential role for co-chaperone Fkbp52 but not Fkbp51 in androgen receptor-mediated signaling and physiology. J Biol Chem 282: 5026–5036 (2007).